

Inositol phosphate production in normal and *Hyp* renal cultures.

Ariane Hsia
Department of Physiology
McGill University, Montreal
March 1997

A thesis submitted to the Faculty of Graduate Studies and Research in partial fulfillment of the requirements of the degree of Master of Science. ©Ariane Hsia, 1997.



National Library
of Canada

Acquisitions and
Bibliographic Services

395 Wellington Street
Ottawa ON K1A 0N4
Canada

Bibliothèque nationale
du Canada

Acquisitions et
services bibliographiques

395, rue Wellington
Ottawa ON K1A 0N4
Canada

Your file *Votre référence*

Our file *Notre référence*

The author has granted a non-exclusive licence allowing the National Library of Canada to reproduce, loan, distribute or sell copies of this thesis in microform, paper or electronic formats.

The author retains ownership of the copyright in this thesis. Neither the thesis nor substantial extracts from it may be printed or otherwise reproduced without the author's permission.

L'auteur a accordé une licence non exclusive permettant à la Bibliothèque nationale du Canada de reproduire, prêter, distribuer ou vendre des copies de cette thèse sous la forme de microfiche/film, de reproduction sur papier ou sur format électronique.

L'auteur conserve la propriété du droit d'auteur qui protège cette thèse. Ni la thèse ni des extraits substantiels de celle-ci ne doivent être imprimés ou autrement reproduits sans son autorisation.

0-612-29717-9

Canada

ABSTRACT

Familial hypophosphatemic rickets and its murine model, *Hyp*, are characterized by a specific defect in renal inorganic phosphate reabsorption. In *Hyp* mice the defect has been localized to the proximal tubule brush border membrane and a constitutively enhanced protein kinase C has been demonstrated. Since the latter is activated through the protein G pathway, we have studied phosphatidyl inositol 4,5-bisphosphate metabolism (PIP₂) in normal (+/Y) and *Hyp* primary cultures of proximal tubules. At confluence, [³H]-myo-inositol labelled cultures were stimulated with calcitriol or parathyroid hormone (PTH) for one minute. Cells were extracted and the aqueous phase was chromatographed on ion exchange resin. The inositol phosphate fractions were counted for radioactivity. For calcitriol, maximal PIP₂ metabolism occurred at 10⁻¹¹ M and 10⁻¹² M for +/Y and *Hyp*, respectively. For both cultures, PTH produced a maximum at 10⁻⁸ M. Pertussis toxin alone stimulated +/Y but not *Hyp* cultures and produced no additive stimulation with calcitriol or PTH in either culture.

RÉSUMÉ

L'hypophosphatémie familiale et la souris *Hyp* sont caractérisées par une diminution de la réabsorption rénale du phosphate. Chez la souris le défaut de réabsorption a été localisé dans la bordure en brosse des tubules proximaux. L'activité de la protéine kinase C est aussi anormalement élevée. La kinase C étant modulé par les protéines G membranaires, nous avons étudié le métabolisme du phosphatidylinositol 4,5-bisphosphate en utilisant des cultures primaires de tubules rénaux de souris normales et *Hyp*. Les tubules, marqués avec [³H]-myo-inositol, ont été stimulés avec le calcitriol ou l'hormone parathyroïdienne (PTH) pour une minute. Les inositols phosphates ont été extraits et chromatographiés sur des colonnes échangeuses d'ions. La radioactivité des différentes fractions a été comptée. La stimulation maximale a été obtenue à 10⁻¹¹ M et 10⁻¹² M en calcitriol pour les tubules normales et *Hyp*, respectivement. Aucune différence n'a été observée lorsque les tubules ont été stimulés par la PTH (10⁻⁸ M). La toxine bordella pertussis a stimulé les cultures normales mais non les cultures *Hyp*. Aucune stimulation additionnelle a été observée en utilisant la toxine avec le calcitriol ou la PTH.

ACKNOWLEDGEMENTS

I would like to thank P. Richard, M. Dussault and A. Arabian for their technical support and their friendship. A special thank you to F. Piccolo and to my parents for reasons too numerous to mention. My gratitude also goes out to B. Ganss, who was the driving force behind seeing me through this project. In addition I would like to thank Dr. E. Delvin for guiding me through this program and for his assistance in the writing of this manuscript. I would also like to acknowledge Dr. E. Cooper and Ms. L. Tracey for their assistance and their patience.

TABLE OF CONTENTS

	Page no.
Abstract	i.
Résumé	ii
Acknowledgements	iii
Table of contents	iv
List of figures	vi
List of tables	vii
List of abbreviations	viii
INTRODUCTION	1-30
I. Phosphate Homeostasis	1
II. Phosphate Excretion	2
III. Renal Phosphate Handling	2
(a) Sites of phosphate transport	4
IV. Adaptive Mechanisms	6
V. Bone Physiology	10
VI. X-linked Hypophosphatemia	12
(a) Clinical features	12
(b) Genetics.	13
(c) Localization of the gene	15
VII. The <i>Hyp</i> Mouse	16
(a) Skeletal findings	16
(b) Intestinal findings	17
(c) Renal findings	18
(d) Vitamin D findings	20
(e) PTH response findings	23
(f) Protein kinase findings	24
VIII. Objectives	25
IX. Phosphatidylinositol 4,5-bisphosphate metabolism	26

MATERIALS	v 31
METHODS	32-34
(a) Renal cell culture	32
(b) Analysis of inositol phosphates	33
RESULTS	35-47
(a) Morphology of confluent cells	35
(b) Metabolism	35
(c) PIP ₂ metabolism	36
(d) Analysis of inositol phosphates	37
DISCUSSION	48-56
CONCLUSION	57
REFERENCES	58-64

LIST OF FIGURES

	Page no.
1. Diagram of a nephron depicting the histological features of the different cell types.	3
2. Schematic representation of transcellular Pi transport.	5
3. A schematic summary of the changes in phosphate and calcium metabolism in response to Pi starvation.	8
4. A schematic summary of the changes in calcium and phosphate metabolism in response to Ca ⁺² starvation.	9
5. Skeletal Preparations from five month old <i>Hyp/Y</i> and <i>+/Y</i> male mice.	17
6. Summary of events in activation of G proteins as a result of ligand binding to its receptor.	29
7. Schematic diagram of agonist stimulated inositol phosphate cascade.	30
8. 25(OH)vitamin D ₃ metabolism by PT enriched cultures from normal and <i>Hyp</i> mice.	36
9. Total pools of [³ H]myo-inositol labelled products from PT enriched cultures from normal and <i>Hyp</i> mice.	39
10. Percent incorporation of [³ H]myo-inositol into IP in PT enriched cultures stimulated with 1,25(OH) ₂ D ₃ for one minute.	40
11. Percent incorporation of [³ H]myo-inositol into IP in PT enriched cultures stimulated with PTH for one minute.	42
12. Percent incorporation of [³ H]myo-inositol into IP in PT enriched cultures stimulated with 1,25(OH) ₂ D ₃ for one minute with or without preincubation with 100 ng/ml PTX for 4 hours.	45
13. Percent incorporation of [³ H]myo-inositol into IP in PT enriched cultures stimulated with PTH for one minute with or without preincubation with 100 ng/ml PTX for 4 hours.	47

LIST OF TABLES

	Page no.
1. Summary of the clinical features and biochemical signs of FHR in early childhood	14
2. Percent incorporation of [³ H]myoinositol into inositol phosphate pools from PT enriched cultures stimulated with 1,25(OH) ₂ D ₃ for 1 minute.	39
3. Percent incorporation of [³ H]myoinositol into inositol phosphate pools from PT enriched cultures stimulated with PTH for 1 minute.	41
4. Percent incorporation of [³ H]myoinositol into inositol phosphate pools from PT enriched cultures stimulated with 1,25(OH) ₂ D ₃ for 1 minute with or without preincubation with PTX for 4 hours.	44
5. Percent incorporation of [³ H]myoinositol into inositol phosphate pools from PT enriched cultures stimulated with PTH for 1 minute with or without preincubation with PTX for 4 hours.	46

ABBREVIATIONS

BBM	Brush Border Membrane
Ca ⁺²	Calcium
25(OH)D ₃	25-Hydroxy Vitamin D ₃
1,25(OH) ₂ D ₃	1,25-Dihydroxy Vitamin D ₃
24,25(OH) ₂ D ₃	24,25-Dihydroxy Vitamin D ₃
DAG	Diacylglycerol
DT	Distal Tubule
ER	Endoplasmic Reticulum
GDP	Guanosine Diphosphate
G _i	Inhibitory G protein
G Protein	Guanyl Nucleotide Binding Protein
G _s	Stimulatory G protein
GTP	Guanosine Triphosphate
HPLC	High Pressure Liquid Chromatography
<i>Hyp</i>	Hypophosphatemia (murine)
IP	1-Inositol Monophosphate
IP ₂	1,4-Inositol Diphosphate
IP ₃	1,4,5-Inositol Triphosphate
IP ₄	1,3,4,5-Inositol Tetrphosphate
K ⁺	Potassium
Na ⁺	Sodium
PCT	Proximal Convoluted Tubule
Pi	Phosphate (inorganic)
PIP ₂	Phosphatidylinositol 4,5-bisphosphate
PKA	cAMP dependent Protein Kinase or Protein Kinase A
PKC	Phospholipid Dependent Protein Kinase or Protein Kinase C
PLC	Phospholipase C
PMA	Phorbol 12-Myristate 13-Acetate
PST	Proximal Straight Tubule
PT	Proximal Tubule
PTH	Parathyroid Hormone
XLH	X-linked Hypophosphatemia
YAC	Yeast Artificial Chromosome

INTRODUCTION

The importance of inorganic phosphate (Pi), a nutrient easily obtained from the diet, should not be underestimated since it is involved in cell metabolism in general and, in that of bone in particular. 85% of the body's Pi is found in bone, primarily as hydroxyapatite (1). Of the remaining 15%, some Pi is found in the blood at a concentration of 1-1.5 mmol/L, almost exclusively as free ion (2). In the blood at pH 7.4 the $\text{HPO}_4^{2-}/\text{H}_2\text{PO}_4^-$ concentration ratio is 4:1 (3). Inorganic phosphate, an integral part of a number of cellular components, being covalently bound to polynucleotides, proteins and phospholipids, is an important element of those biological structures.

It follows that disturbance of phosphate homeostasis, whether it be acquired or inherited, results in cellular dysfunction and ultimately into diseases of which X-linked hypophosphatemia (XLH) is an example. Before treating of this condition, a brief review of phosphate homeostasis will be presented. Calcium will also be dealt with, since a close link exists between it and phosphate in areas such as renal transport, bone physiology and vitamin D metabolism.

I. PHOSPHATE HOMEOSTASIS:

The major factors governing Pi homeostasis are the amount acquired from the diet, the efficiency of absorption in the intestine and reabsorption by the kidney. A normal diet provides to an adult human 800 to 1600 mg of phosphate per day, thereby easily fulfilling the recommended daily allowance of 800mg/day (2). Pi is absorbed from the diet with an average efficiency of 70%. However upon decrease in dietary availability, adaptive mechanisms lead to

an increase in absorption up to 90% (4).

Phosphate is consumed in both organic and inorganic forms. Most organic phosphate compounds undergo conversion to Pi, which is the form readily absorbed. Pi is absorbed by the jejunum and the ileum through active and passive processes (5). Some absorption also occurs in the duodenum, albeit at a much lower rate, while no absorption takes place in the colon (6).

The metabolically active form of vitamin D, 1,25(OH)₂ vitamin D₃ (1,25(OH)₂D₃), does not play a major role in regulating Pi absorption. However, it is thought that the minor increase in Pi absorption in response to 1,25(OH)₂D₃, is secondary to the hormone's effect on calcium (Ca⁺²) absorption from the intestinal tract. Thus it could be conceived that Ca⁺² may act as a transport mediator for Pi (7).

II. PHOSPHATE EXCRETION:

Some Pi is excreted in the feces in combination with Ca⁺². However most of the ingested Pi is transported to blood from the intestine. Phosphate obtained from metabolism and that absorbed from the intestine is excreted in the urine (7). Plasma concentration of Pi remains constant due to adaptive renal mechanisms (7). Thus if plasma Pi concentration falls below 1 mmol/L, complete reabsorption occurs with no urinary Pi excretion (7). Above this threshold, Pi excretion becomes proportional to the plasma phosphate load.

III. RENAL PHOSPHATE HANDLING:

The apparatus responsible for the majority of phosphate handling is the nephron (figure 1).

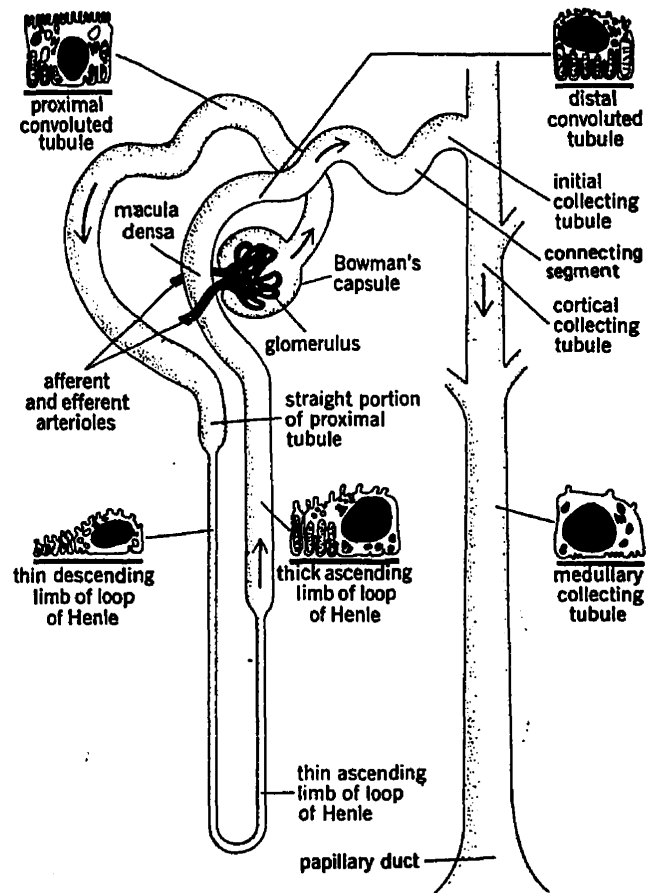


Figure 1. Diagram of a nephron depicting the histological features of the different cell types. IS:inner stripe, OS:outer stripe (8).

The nephron is composed of a single layer of epithelial cells resting on a basement membrane (8). The structure and function of these various epithelial cells vary greatly from segment to segment of the nephron. One common characteristic of these epithelial cells is the presence of tight junctions between adjacent cells (8). Each nephron is composed of a filtering component, the glomerulus, and a tubule extending out from the glomerulus. The glomerulus consists of Bowman's capsule and it is into this that fluid is filtered from the glomerular capillaries. The capsule is followed by the proximal tubule (PT) which is divided into the convoluted portion or pars convoluta followed by a straight segment or pars recta. The pars recta then drains into the thin descending limb of the loop of Henle. This segment is followed

by the thin ascending limb of the loop of Henle. In nephrons with very long loops, the thin ascending limb is followed by the thick ascending limb of the loop of Henle. The distal tubule which follows is made up of the distal convoluted tubule, the connecting segment and the initial collecting tubule (8).

Renal handling of Pi involves glomerular filtration. This process is followed by partial tubular reabsorption which depends, at steady state, on the load. Secretion is not believed to be involved in the renal processing of Pi (9).

(a) Sites of phosphate transport:

Phosphate transport systems are located in two distinct anatomical sites in the proximal tubule. Renal Pi transport is a transcellular, carrier mediated, saturable process of which the proximal convoluted tubule (PCT) is the main site since it accounts for 60% of reabsorption of the filtered load (10). The proximal straight tubule (PST) is responsible for an additional 20%.

The early PCT has two Pi transport systems (11). The first is a low affinity and high capacity system responsible for the bulk of the reabsorption and, the second is of high affinity and low capacity responsible for the reabsorption of the remaining Pi. On the other hand the PST has a single, high affinity system.

Parathyroid hormone (PTH) is known to regulate many renal functions, among which are the inhibition of Na^+/H^+ exchange in the PCT, stimulation of Ca^{+2} reabsorption in the distal tubule (DT) and regulation of Pi reabsorption in the PCT (only the high affinity/low capacity system) and the PST(5). A summary of the mechanism of Pi transport is shown in figure 2.

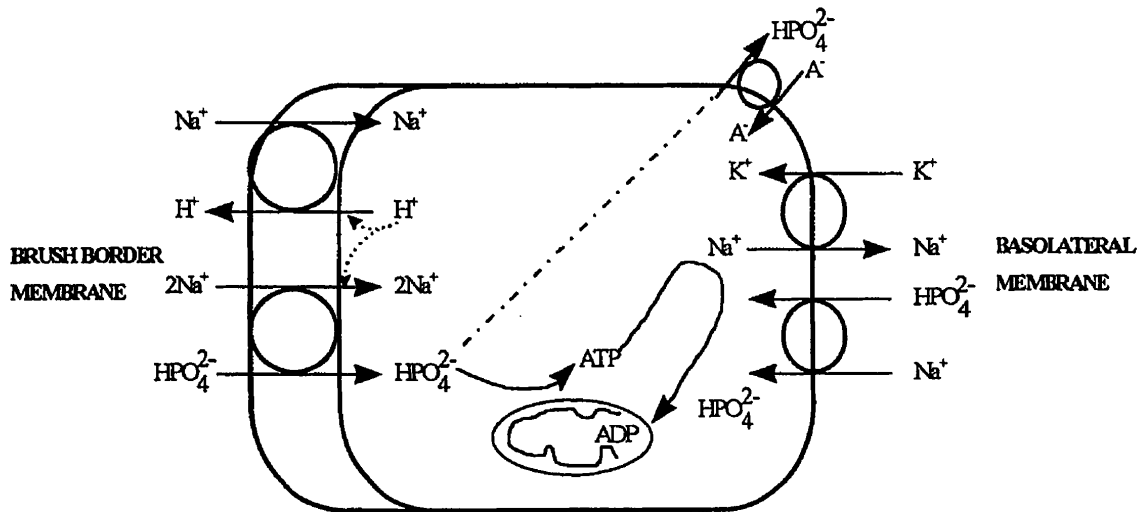


Figure 2. Schematic representation of transcellular Pi transport (5).

Unidirectional Pi transport flows from the brush border membrane (BBM) at the lumen of the nephron to the basolateral membrane. Pi, in the form of HPO_4^{2-} , is transported by secondary active transport which is driven by a sodium (Na^+) gradient. This $\text{Na}^+/\text{HPO}_4^{2-}$ cotransporter allows two Na^+ cations to enter the cell for each HPO_4^{2-} in an electroneutral process. When the predominant species is H_2PO_4^- , the process becomes electrogenic (5). Since this Pi transport depends on the Na^+ gradient, this cation must be removed from the cell to maintain the Na^+ concentration gradient between the lumen and the cell. The Na^+ is pumped out of the cell via a sodium/potassium (K^+) ATPase found in the basolateral membrane. The cell becomes depleted of sodium so that Na^+ and Pi can be brought across the BBM. The importance of the sodium gradient is proven by the inhibition of Pi transport when an Na^+/K^+ ATPase inhibitor is used to prevent the maintenance of the sodium gradient (5). The intracellular Pi exits the cell across the basolateral membrane. This efflux is driven by the

electrical gradient that exists across this membrane and occurs by an anion exchange mechanism. There is also secondary Na^+ -linked influx of Pi across the basolateral membrane, with a V_{max} of only 10 % of the luminal process (5). In the absence of luminal Pi movement, this influx is not capable of maintaining a normal intracellular Pi concentration. Due to the continuous entry and exit of Pi into and out of the cell, intracellular Pi is difficult to measure. A value of 0.7mM has been obtained with the use of NMR spectroscopy (12). A concentration range of 0.6mM to 1.0 mM is thought to be a reasonable estimate.

IV. ADAPTIVE MECHANISMS:

Three scenarios will be presented: in the healthy individual extreme Pi deprivation rapidly leads to an abrupt reduction in renal Pi excretion (5). Within a few days of limited intake, urinary Pi excretion is completely abated and Pi reabsorption and Ca^{+2} excretion increase. As a result of these adaptive processes, the decrease in plasma Pi concentration over these few days is minimal. However if starvation conditions persist, the plasma Pi level drops (5). Changes in Pi tubular transport as well as those in plasma Pi concentration enhance an elevation in proximal tubule 25(OH)vitamin D_3 1- α -hydroxylase activity, leading to an increase in 1,25(OH) $_2\text{D}_3$ plasma concentration. The increased concentration of 1,25(OH) $_2\text{D}_3$ in turn contributes, in conjunction with PTH, to the stimulation of bone resorption shifting Pi and Ca^{+2} from mineralized bone to extracellular fluids (13). As plasma Pi and Ca^{+2} levels begin to rise, PTH secretion is repressed. It must be stressed at this point, that PTH synthesis and secretion is also under the control of 1,25(OH) $_2\text{D}_3$ (13). The falling PTH concentration leads to a decrease in distal tubular reabsorption of Ca^{+2} and hence to an increase of Ca^{+2} excretion (5). Thus there is a balance between increased Ca^{+2} coming from bone and gut and increased renal loss. The

diminishing amount of PTH does not increase Pi reabsorption contrary to what is expected. Indeed the Pi transport system in Pi deprived organisms has been shown to be insensitive to this action of PTH (5). The kidney desensitization to the peptide hormone has been documented by experiments in which infusion of PTH to Pi deprived rats did not stimulate urinary Pi excretion as it did in control fed animals (5).

An increase in Na^+/Pi cotransport has also been reported in the kidney BBM vesicles isolated from rat, mouse, rabbit and human (14-18). Two to four hours after limiting Pi ingestion, the plasma Pi concentration remains largely unchanged yet the increase in Pi transport begins to adapt. A 3 to 5 fold increase in V_{max} is eventually reached (15). The early modification in Pi transport, precludes de novo synthesis of cotransporters. Using the kidney cell line LLC-PK₁, Biber et al. (19) and Caverzasio et al. (20) have elegantly shown that during the early phase of the increase in Pi transport, preformed Na^+/Pi cotransporter molecules from the intracellular vesicular pool are inserted into the BBM. These groups have found that adaptation to low Pi occurs in two phases, a rapid one increasing the rate of Pi transport by ~30% within 10 minutes and a slow phase that doubles Pi transport after 15 hours. The initial rapid adaptation is unaffected by treatment with cycloheximide and actinomycin D, thereby suggesting that the increase in Pi transport is due to preformed co-transporters. The slow phase is on the other hand, affected by these inhibitors therefore confirming the need for de novo synthesis of cotransporters for long term adaptation (19, 20).

The adaptive response of the normal individual to Pi deprivation is illustrated in Figure 3.

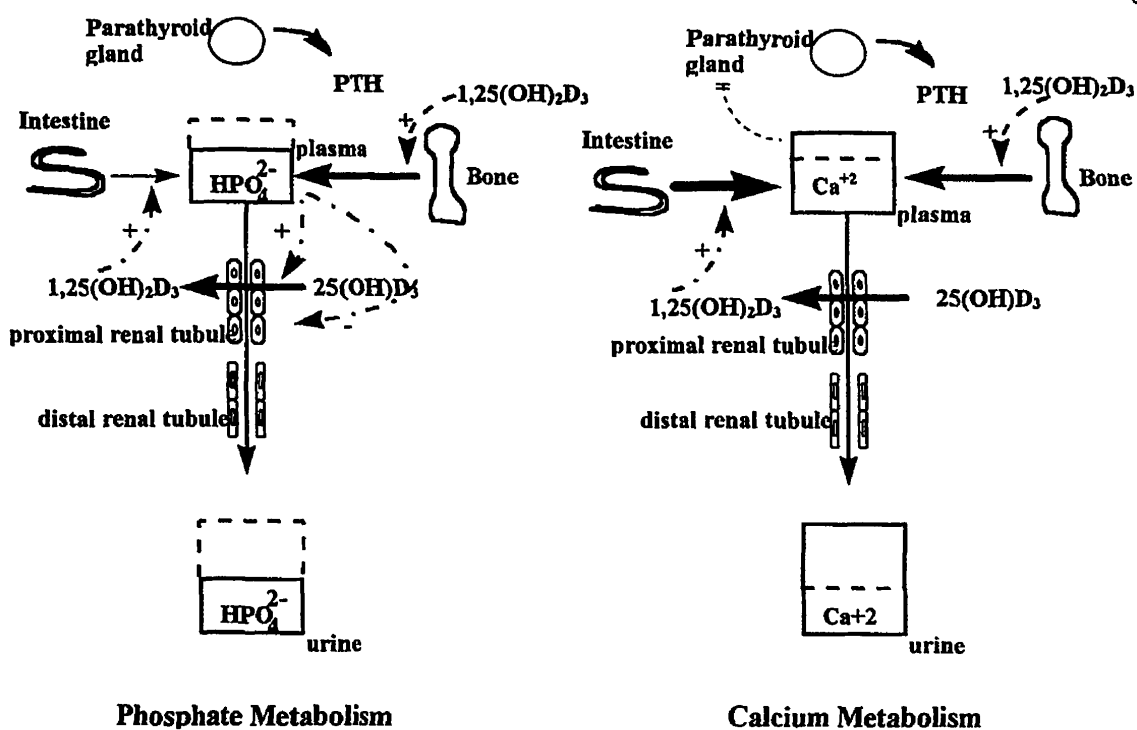


Figure 3. A schematic summary of the changes in phosphate and calcium metabolism in response to Pi starvation. (5)

However, if the normal organism is fed a Pi enriched diet, renal Pi excretion will increase to counterbalance the overload. As a result the plasma Pi concentration remains largely unaffected. However, plasma Pi may rise enough (especially if the dietary Pi excess is associated with low Ca^{+2} intake) to reduce the plasma level of calcium (5). This calcium reduction stimulates PTH release which in turn further limits Pi reabsorption. In this scenario, PTH generates less of an elevation in $1,25(\text{OH})_2\text{D}_3$. Thus it is important to note that supplementing the diet with excess Pi as a therapeutic tool can lead to secondary hyperparathyroidism (5).

Lastly Ca^{+2} restriction, leads to a slight fall in plasma calcium which stimulates PTH synthesis and secretion. The higher level of circulating PTH in turn increases bone resorption, distal tubular reabsorption of Ca^{+2} and of $1,25(\text{OH})_2\text{D}_3$ synthesis by the proximal tubule. This

newly synthesized active vitamin D stimulates intestinal Ca^{+2} absorption and acts in conjunction with PTH to amplify Ca^{+2} resorption from bone (5). Pi is also absorbed in the intestine and lost from bone due to the action of $1,25(\text{OH})_2\text{D}_3$. The PTH also inhibits renal tubular Pi transport to a certain degree. This inhibitory action leads to a decrease in the concentration of Pi in the plasma. As a result of restricted Ca^{+2} intake, the newly reached balance delivers efficient Ca^{+2} conservation with resorption of skeletal Ca^{+2} to counteract loss of Ca^{+2} from the gut (5). A summary of the above events is represented in figure 4.

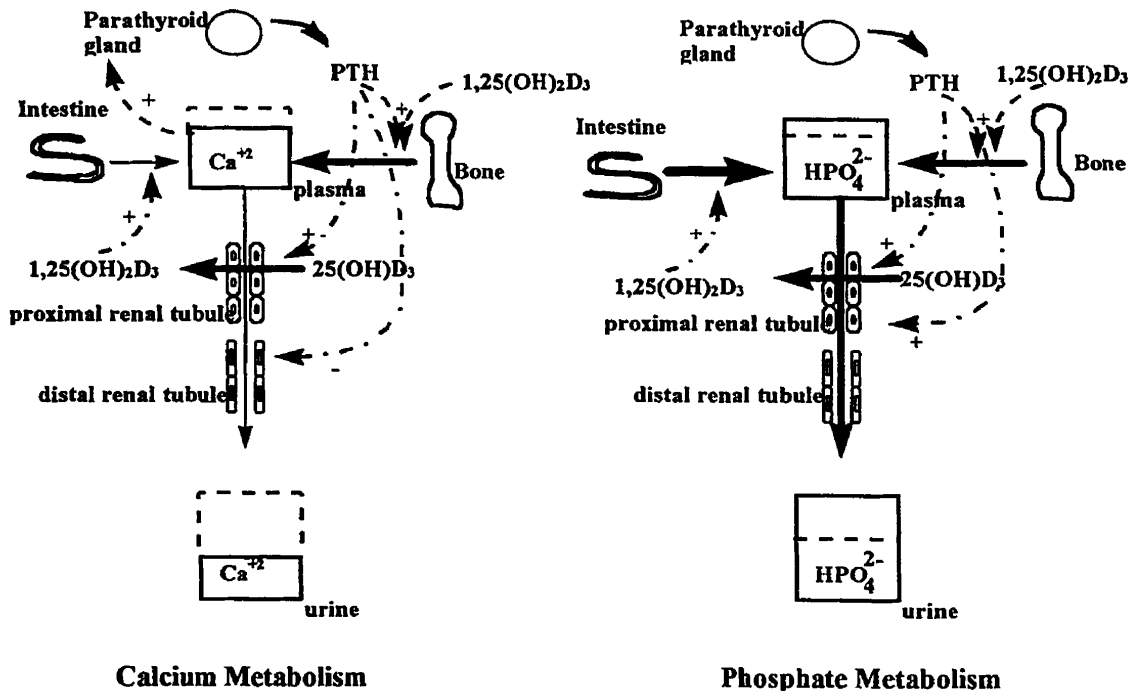


Figure 4. A schematic summary of the changes in calcium and phosphate metabolism in response to Ca^{+2} starvation. (5)

V. BONE PHYSIOLOGY:

Pi, in the form of hydroxyapatite, is an integral part of mineralized bone. As bone undergoes continuous remodelling, Pi in conjunction with Ca^{+2} , is either deposited in bone or resorbed from bone in dynamic processes which will be briefly described.

Bone serves several very important functions. It provides mechanical support and sites for muscle attachment, it protects the vital organs and bone marrow and also functions as a metabolic reserve of ions, particularly Ca^{+2} and Pi (21).

Bone formation and bone resorption are regulated by two principal cell types. Osteoblasts, responsible for the formation of bone, synthesize necessary structural proteins such as collagen proteoglycans and other non-collagen proteins upon which Ca^{+2} and Pi crystallize to form hydroxyapatite (1, 21). The osteoblast becomes surrounded by bone tissue and is transformed to an osteocyte. Although osteocytes are not able to synthesize large amounts of bone, they most likely play an important part in mineral homeostasis. Osteoclasts on the other hand, solubilize and resorb previously formed bone, thereby releasing ions (1). Once bone is fully grown, remodelling is continuously taking place. This process, essential to mineral homeostasis, is characterized by the coupling of osteoblast and osteoclast activities. First, osteoclasts are recruited to a site on the bone surface. The osteoclast then typically resorbs bone to a depth of $50\mu\text{m}$ (1). Osteoblasts then replace the osteoclasts at the site and new bone is deposited in the space. With age the osteoblasts are unable to completely replace the volume of resorbed bone, resulting in conditions such as osteoporosis. The activities of these bone forming and resorbing cells are regulated by a number of humoral and circulating factors among which are PTH and $1,25(\text{OH})_2\text{D}_3$ (1). These processes are usually in equilibrium.

PTH causes bone resorption by acting indirectly on the osteoclasts since these do not possess PTH receptors. PTH causes changes in the function and phenotype of osteoblasts (1). In osteoblasts, PTH governs ion and amino acid transport, stimulates cAMP and regulates collagen synthesis. (22-24). These PTH activated osteoblasts, via cytokines, then cause the formation of mature, multinucleated osteoclasts, which carry out their function and cause bone resorption. Bone resorption causes release of calcium, phosphate and matrix components such as collagen. Although phosphate is released from bone PTH actually leads to a decrease in the Pi blood level, due to the phosphaturia caused by PTH. The low levels of Pi accentuate the effect of PTH since the decrease in Pi also leads to bone resorption (1).

$1,25(\text{OH})_2\text{D}_3$ is needed for normal growth and bone mineralization but it does not stimulate bone formation directly. Like PTH, $1,25(\text{OH})_2\text{D}_3$ acts indirectly on the osteoclast population and stimulates bone resorption (1). $1,25(\text{OH})_2\text{D}_3$ enhances the synthesis of osteocalcin, a peptide known to be synthesized only by osteoblasts. Therefore $1,25(\text{OH})_2\text{D}_3$ has direct stimulatory effects on osteoblasts. Although it is believed that the released osteocalcin is needed for osteoclast recruitment and bone formation, its exact function in bone remodelling is not yet known (25). It is also interesting to note that in the absence of $1,25(\text{OH})_2\text{D}_3$, PTH cannot efficiently cause bone resorption (1). The mechanism for this action also remains elusive.

It is important to keep the regulatory roles of hormones such as PTH and $1,25(\text{OH})_2\text{D}_3$ in mind when considering Pi homeostasis. As described earlier, $1,25(\text{OH})_2\text{D}_3$ is synthesized in times of Pi deprivation. This increase in $1,25(\text{OH})_2\text{D}_3$ leads to bone resorption which causes a shift of Pi from the skeleton to the extracellular fluid, thereby correcting the drop in Pi plasma concentration. Should the lack of dietary Pi persist, then the equilibrium between bone

deposition and reabsorption will shift in favour of a net loss of bone mass (1). For a complete discussion of bone physiology the reader is referred to reference 1.

Now that the physiological considerations of Pi homeostasis and handling are summarized, the effect of XLH, an inherited lesion of Pi transport, will be discussed.

VI. X-LINKED HYPOPHOSPHATEMIA:

With the background knowledge of the normal adjustments that take place in response to dietary restrictions, it is now possible to go on to understand what is amiss in XLH.

(a) Clinical features:

XLH, an X-linked dominant disease, is the most common form of inherited vitamin D resistant rickets in humans (26). Among the visible abnormalities are short stature and femoral and tibial bowing. XLH patients have normal muscle tone and show no sign of tetany or convulsions (26). These manifestations of the disease appear during the first 2 years of life. The disease is difficultly diagnosed within the first half year since physical signs are minimal and plasma Pi concentration may remain normal. However, plasma alkaline phosphatase is elevated during this period. A more accurate diagnosis can be made after 1 year of age as some stunting of growth is visible. Hypophosphatemia and high plasma alkaline phosphatase also become evident. Signs of XLH are also detectable by X-ray (widened epiphyseal plate and decreased mineralization) (26). Classical, clinical features are also spontaneous tooth abscesses and late dentition. Children are also more prone to fractures, a symptom not seen in the adult. Once the bones are fully grown, alkaline phosphatase levels are normal although osteomalacia remains if the patient remains untreated. However bone pain is reported to occur in some patients which

may be the result of bone overgrowth (26).

Low plasma Pi concentration is characteristic of XLH. As described earlier, normal individuals, in response to restricted Pi intake, exhibit an increase in $1,25(\text{OH})_2\text{D}_3$ (27). However, in XLH no such response is seen. In fact, the level of $1,25(\text{OH})_2\text{D}_3$ is normal while plasma calcium is in the low to normal range with reduced urinary calcium excretion (27).

Based on studies using biopsy material from six patients affected by X-linked hypophosphatemia, Glorieux et al. (28) have shown the Pi uptake by human jejunal mucosa does not significantly differ from the normal individual. Thus the Pi transportation defect appears to be restricted to the kidney. A summary of the symptoms of XLH is shown in table 1.

(b) Genetics:

XLH is an X-linked dominant disorder (26). Whereas affected males nearly always have clinically evident bone disease, half of females do not (26). The reason for this difference does not lie in the degree of hypophosphatemia since XLH women and men have the same range of plasma Pi concentrations. It is postulated that the gene responsible for XLH is governed by X chromosome inactivation also known as the Lyon hypothesis (29). Although the exact mechanisms presiding over the HYP gene inactivation remain unclear at the present time, X chromosome inactivation has been shown to occur in both X-linked (as is the case for XLH) and autosomal genes (29). This inactivation is a type of gene regulation in which selected parts of a chromosome are shut down during early embryogenesis of the female (29).

FAMILIAL HYPOPHOSPHATEMIC RICKETS	
Inheritance	X-linked
Age of onset	Early childhood
Clinical features	
short stature	++
bone pain	++
femoral bowing	++
muscle weakness	-
Radiologic signs	
rickets	++
pseudofracture	+
coarse trabeculi	++
Dental abnormalities	++
Calcium metabolism	
serum Ca ⁺²	N-LN
iPTH	N-HN
Ca (urine)	L
Ca absorption	L
Phosphate metabolism	
serum phosphate	L
TmP/GFR	L
alkaline phosphatase	H
Vitamin D metabolism	
25(OH)D ₃	N
1,25(OH) ₂ D ₃	N-LN
25(OH)D ₃ 1- α hydroxylase response to phosphate	Abnormal

iPTH =immunoreactive parathyroid hormone;L= low; N= normal;
LN = low normal; H=high; HN= high normal

Table 1. Summary of the clinical features and biochemical signs of XLH in early childhood. Note the presence of high alkaline phosphatase which later returns to normal levels in adulthood (5).

Genes that escape inactivation are interspersed with those subjected to inactivation on the chromosome. Also responsible for the difference between male and female XLH patients may be the phenomenon of imprinting. Maternal and paternal imprinting adds additional information to the inherited genomes, information that may regulate gene activity and chromosome behavior (30). A mutant gene may cause lethal defects if inherited from one parent but does not produce these deficiencies if inherited from the other. The severity of the disease seen in females may depend upon whether the gene is inherited from the maternal or the paternal side,

thereby providing a possible explanation for the lack of bone disease in many XLH afflicted females. An example of such a parentally imprinted gene is that of human *IGF2*, in which inheritance occurs from the paternal side (31).

(c) Localization of the gene:

Genetic linkage analysis has led to the localization of the gene responsible for XLH to the distal portion of Xp (Xp22.1 region) (32). Subsequently, the genetic map was updated to include DXS257 and DXS365 as established telomeric markers (33). Further investigation established that DXS365 is the closest to the gene locus, that is, it is the closest telomeric flanking marker (34). This study also concluded that DXS274 is the nearest flanking marker on the centromeric side of the gene, with the estimated distance between DXS365 and DXS274 being approximately 3.5cM (34). Recent studies describe the development of a yeast artificial chromosome (YAC) contiguous map for the area encompassing DXS365 to DXS274 (35). This study concluded that DXS365 and DXS274 are 1 Mb apart. A more recent study used this same YAC contiguous map to investigate DXS1683 which lies between DXS365 and DXS274 (36). It was discovered that the HYP gene actually lies between DXS365 and DXS1683. The distance between these two markers is now only 350 to 650 kilobases, further reducing the area to be studied to localize the HYP gene.

Recently, a candidate gene has been isolated by positional cloning from the HYP region in XP22.1 (37). This gene (named PEX) is thought to be a novel member of a family of endopeptidase genes which are responsible for degradation or activation of a variety of peptide hormones. In HYP patients, four deletions and three mutations within PEX support the notion that this gene is involved in HYP (37). These deletions and mutations most likely result in the

loss of function of the PEX gene product. The mechanism by which PEX would control phosphate homeostasis has not been described. It is thought that PEX may act enzymatically on a hormone that regulates renal phosphate handling.

VII. THE HYP MOUSE:

Since studies on humans are limited, it is fortunate that an animal model for XLH was discovered. In 1976 a new mutation in the laboratory mouse was reported to be the murine model for the human disease of XLH (38). This *Hyp* model is thought to be the evolutionary homologue to XLH in man since their phenotypes are almost indistinguishable. The following manifestations of the disease were also found in the mouse (38):

- hypophosphatemia without hypocalcemia
- same relative time of appearance of clinical features after birth
- bone disease and dwarfism
- high urinary excretion of Pi relative to serum Pi
- lack of hyperparathyroidism as would be expected in the unaffected mouse fed a low Pi diet.

Thus based on the similar pattern of X-linked dominant inheritance and similar phenotypes, it was concluded that the *Hyp* mouse was a suitable model for XLH.

(a) Skeletal findings:

In matings of *Hyp*/+ females with +/Y males, heterozygous female and hemizygous male offspring can be separated from their normal siblings at 21 days of age based on their shortened limbs and tail (38). Reduced body weight and size are also apparent. Features, such as bowing of the femur, become more apparent with age. As in humans, most skeletal deformities are more pronounced in the male than in the *Hyp*/+ female (38). The main distinction between the disease in humans versus mice is that the bone disease is worse in the

mice. The skeletal differences between the normal and affected mouse are illustrated in figure 5.

The shorter vertebral length in the *Hyp* model is associated with a wider epiphyseal growth plate (38). In affected females, the femora increases its mineral content with age whereas the male shows no further increase after 15 weeks of age.

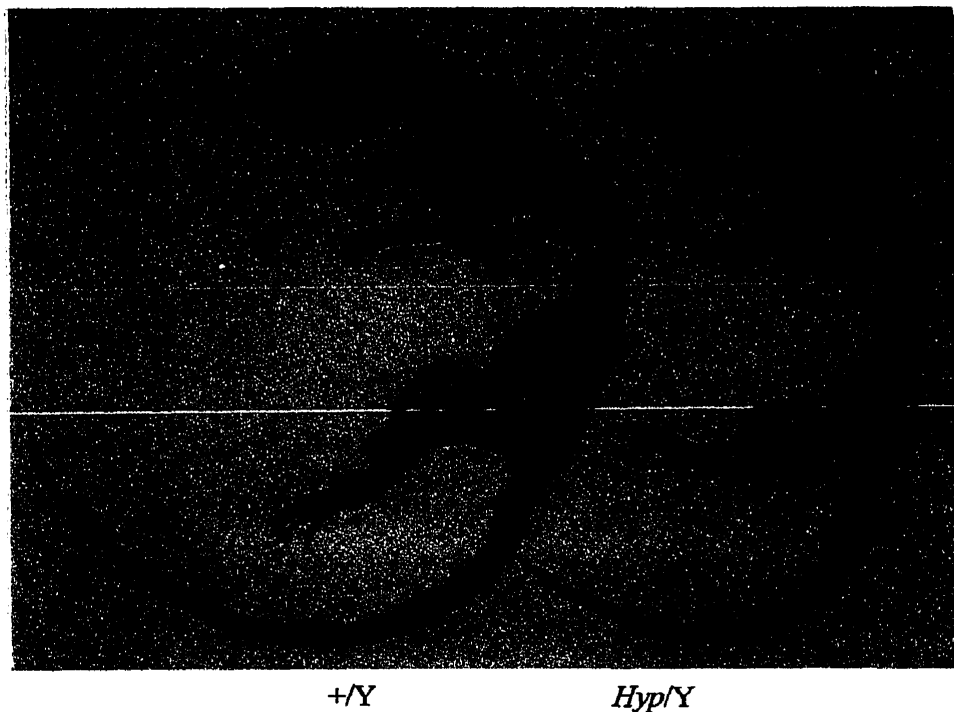


Figure 5. Skeletal preparations from five month old $+/Y$ and *Hyp/Y* male mice. The mutant mouse is smaller and shows characteristic kyphosis of the spine as well as shorter limbs and tail as reported by Eicher et al. (38).

It was also observed that heterozygous females were fertile whereas not all hemizygous males are (5).

(b) Intestinal findings:

In BBM isolated from the jejunum of both strains of mice, no difference was found in Na^+ dependent Pi transport or in glucose transport (39). In addition, the $1,25(\text{OH})_2\text{D}_3$ receptor in the intestine of both genotypes displayed the same agonist affinity and receptor number (40). This finding, along with the result that intestinal vitamin D dependent Ca^{+2} binding proteins are

identical in *Hyp* and normal mice, speak against an intestinal resistance to $1,25(\text{OH})_2\text{D}_3$ in the hypophosphatemic mouse (41).

(c) Renal findings:

As in XLH, Pi transport and renal excretion increase in the mutant mouse with increasing plasma Pi concentration. Micropuncture studies have localized the Pi transport defect to the proximal tubule of the *Hyp* renal nephron (42).

It is still not known whether the mutant renal phenotype is intrinsic to the kidney or whether it is due to an inappropriate expression of a humoral factor. Data have been obtained to support both theories. It was found *in vitro* that confluent monolayers of proximal tubule cells from the mutant mouse exhibit a reduced Na^+ dependent Pi/ Na^+ dependent α -methyl glucoside transport ratio (43). The ability of the transport defect to be detected in cultures of proximal tubule cells, points to an intrinsic problem since these renal cells are removed from their natural environment of circulating humoral factors. The localization of the transport defect was narrowed down further by the discovery that Pi uptake was not impaired in renal cortex slices. In these slices, it was the basolateral surface of cells which was chiefly exposed. Such observations suggested that Pi transport across the basolateral membrane was normal (44). Further investigation of purified BBMs demonstrated that the *Hyp* mouse had impaired sodium dependent Pi transport at the BBM (44).

In order to verify that the BBM defect was specific for the kidney, a study was conducted to compare BBM vesicles from kidney to those from the intestine in normal and mutant mice. Pi uptake in normal and *Hyp* mice was the same for BBM from the intestine (16). However the V_{max} for Pi uptake was once again lower in renal BBM from hypophosphatemic

mice when compared to normal mice. This same study also verified that the defect was not a generalized one, but one specific for Pi, by demonstrating that α -methyl-D-glucose (transported by the BBM Na^+ /glucose transporter) was equally expressed and free of abnormality in renal BBM from normal and *Hyp* mice (16).

As already described, the Pi transport system in the proximal tubule is broken down into two components of high and low capacity. In order to test the adaptive response, a study using phosphonoformic acid, a competitive inhibitor of both Pi systems, was conducted on normal and *Hyp* mice given balanced or Pi poor diets. It was found that the mutation impairs only the high affinity, low capacity process (45). This impaired process had half the normal V_{max} with no change in apparent affinity for Pi (45). Many theories have been investigated in order to shed some light on the source leading to the low V_{max} of the high affinity Na^+ /Pi cotransporter. Impaired response of the transporter to the Na^+ gradient driving force, different membrane potential, external pH and modification of the renal BBM lipid composition have all been discounted as the cause (46). The fairly recent availability of specific cotransporter probes (NaPi-2 cloned from rat and NaPi-3 cloned from human kidney cortex) have facilitated further investigation. The NaPi-2 cDNA is expressed only in the kidney just as the Pi transport defect is expressed only in the kidney (46). This finding supports the notion of an intrinsic kidney defect. Using the specific probes, the defect in sodium dependent Pi transport in renal BBM from mutant mice was shown to be associated with a specific decrease in the renal abundance of Na^+ /Pi cotransporter mRNA and protein (46). The magnitude of the decrease in mRNA was in fact consistent with the decrease in V_{max} (46). With less protein synthesis, the BBM had less high affinity Na^+ /Pi cotransporter sites. Thus the defective cotransporter was suggested to be the gene product from the *Hyp* locus.

However, the cotransporter gene has been found on human chromosome 5q35. This gene not being on the X chromosome, eliminates the possibility that the Na^+ /Pi cotransporter is the gene responsible for X-linked hypophosphatemia (47). It was suggested that the gene at the *Hyp* locus decreases transcription of the cotransporter, thus explaining the lower mRNA levels found (47).

Mutant and normal mice were shown to adapt to Pi deprivation in the same manner but to different degrees. Both sets of mice demonstrated a decrease in renal Pi excretion after two weeks on a Pi restricted diet. There was also an increase in Na^+ dependent Pi transport in both genotypes. However, Pi uptake into BBM vesicles was still much lower for Pi deprived *Hyp* mice than for Pi deprived normal mice (5).

(d) Vitamin D findings:

Regulation of renal $25(\text{OH})\text{D}_3$ 1- α -hydroxylase is impaired in *Hyp* mice just as it is in humans with XLH. Pi deprivation is known to be a potent stimulus for this hydroxylase in the normal mouse (48). The production of $1,25(\text{OH})_2\text{D}_3$ is significantly lower in mutant mice than that found in normal mice with the same degree of hypophosphatemia induced by a low Pi diet. *Hyp* mice also display a noteworthy blunted $25(\text{OH})\text{D}_3$ 1- α -hydroxylase response when challenged with vitamin D or Pi deprivation. The reduced synthesis of $1,25(\text{OH})_2\text{D}_3$ is associated with a decrease in the V_{max} for the $25(\text{OH})\text{D}_3$ 1- α -hydroxylase (48). When compared to control mice, mutant mice once again exhibited a significantly lower hydroxylase response to PTH infusion and to calcium restriction. The murine model parallels the human disease since patients with XLH also produce a blunted $25(\text{OH})\text{D}_3$ 1- α -hydroxylase response to decreased plasma Pi concentrations and to PTH supplementation (49, 50).

The ongoing area of debate of intrinsic defect to the kidney or circulating humoral factors was further investigated by Bell et al. This group examined Pi transport and $25(\text{OH})\text{D}_3$ metabolism in PT enriched cultures from normal and *Hyp* mice. Their findings of decreased Pi uptake and increased $24,25(\text{OH})_2\text{D}_3$ in *Hyp* cultures, support the hypothesis of intrinsic renal defects of Pi transport and vitamin D metabolism in X-linked hypophosphatemia (43). Once again pointing in favour of an intrinsic renal defect is the study carried out by Fukase et al. (51) on primary cultures of renal cortical cells from normal and *Hyp* mice. This study concluded that control of $25(\text{OH})\text{D}_3$ - α -hydroxylase activity is abnormal in *Hyp* mice (51).

Yamaoka et al. (49) have found that normal mice fed a Pi rich diet showed no significant change in $1,25(\text{OH})_2\text{D}_3$ synthesis. However, *Hyp* mice on this same diet exhibited a marked increase in renal $1,25(\text{OH})_2\text{D}_3$ production, demonstrating that the regulation of $25(\text{OH})\text{D}_3$ - α -hydroxylase is abnormal in mutant mice (49).

In a study by Econs et al. (52), evidence supporting the existence of two separate and distinct $25(\text{OH})\text{D}_3$ - α -hydroxylase systems in the *Hyp* mouse was discovered. While one such hydroxylase in the PCT is regulated by PTH, the other, in the PST, is governed by calcitonin. Activity in the PST has been demonstrated to be normal. These findings could be extended to humans since in patients with XLH given calcitonin, increases in calcitriol levels were comparable to those seen in unaffected individuals (52). The same type of study conducted in mice has shown that calcitonin infusion in normal and *Hyp* mice gave equivalent increases in enzyme activity with no significant differences in time course or dose dependency (53). Since defective Pi transport occurs in the PCT it is not surprising that the PCT may also be the site of abnormal $1,25(\text{OH})_2\text{D}_3$ metabolism (53). Later studies examined the effects of PTH and PTH related peptide (PTHrp) on $25(\text{OH})\text{D}_3$ - α -hydroxylase (54, 55). It is known that PTHrp and

PTH share the same receptor. Like PTH, PTHrp regulates 25(OH)D₃1- α -hydroxylase in the PCT but likely by a different pathway than PTH (54). The study showed that although enzyme activity increased in both mutant and normal mice treated with PTHrp, the increase was lower in the mutant mice. The identical response was seen for PTH. In addition, simultaneous infusion of maximally effective doses of PTH and PTHrp gave an additive increase in hydroxylase activity, thereby providing evidence for the existence of different pathways for enzyme activation (54). These observations are indicative of a generalized defect in responsiveness of the PCT to multiple hormones exerting their action by different pathways (54).

The 25(OH)D₃24- α -hydroxylase has also been scrutinized in the *Hyp* mouse. This enzyme is able to hydroxylate 1,25(OH)₂D₃ to its inactive metabolite 1,24,25(OH)₃D₃ and the precursor 25(OH)D₃ to 24,25(OH)₂D₃. The enzyme shows ten times greater affinity for the active form of vitamin D than for its precursor, 25(OH)D₃ (56). Due to its catabolic powers, this hydroxylase is an important regulator of circulating levels of 1,25(OH)₂D₃. Tenenhouse et al. (56) have shown that an altered vitamin D₃ catabolic pathway exists in which renal 24-hydroxylation of vitamin D₃ in *Hyp* mice was twice that of normal mice and that infused 1,25(OH)₂D₃ was cleared from the plasma more rapidly than in normal mice.

Contrary to what should happen when challenged with a low Pi diet (increased 1,25(OH)₂D₃ production and inhibition of 25(OH)D₃24- α -hydroxylase activity), mutant mice show a decrease in circulating 1,25(OH)₂D₃ concentration (57). The renal catabolic pathway has been shown to play a more significant regulatory role on the plasma concentration of 1,25(OH)₂D₃ in the mutant than in normal mice where the synthesis of 1,25(OH)₂D₃ plays the regulatory role (58). Thus, in mutant mice, it is the greater 25(OH)D₃24- α -hydroxylase activity

that causes the decrease in $1,25(\text{OH})_2\text{D}_3$. This increase in enzyme activity is not seen in normal mice on a Pi restricted diet. The increase in renal $25(\text{OH})\text{D}_324\text{-}\alpha$ -hydroxylase activity has been confirmed by demonstrating that there is upregulation of mRNA proportional to the increase in V_{max} for the enzyme (57). As was seen with the Na^+/Pi cotransporter gene, the gene for this 24 -hydroxylase is not found on the X-chromosome and thus cannot be responsible for the abnormality in *Hyp*. The gene has been mapped to an autosome (20q13) in humans. As with the Na^+/Pi cotransporter gene, the most likely explanation is that the gene product at the X-linked *Hyp* locus regulates the expression of the $25(\text{OH})\text{D}_324\text{-}\alpha$ -hydroxylase and does so in an inappropriate manner in times of reduced Pi intake (57). Upregulation of the $25(\text{OH})\text{D}_324\text{-}\alpha$ -hydroxylase enzyme in response to Pi deprivation is specific to the kidney. No 24 -hydroxylase mRNA was found in the duodenum or liver of *Hyp* mice fed the Pi poor diet (57).

One investigation was undertaken to see if the response to regulators known to inhibit renal $25(\text{OH})\text{D}_31\text{-}\alpha$ -hydroxylase and stimulate $25(\text{OH})\text{D}_324\text{-}\alpha$ -hydroxylase was abnormal in the *Hyp* mouse. The inhibitory control of the $25(\text{OH})\text{D}_31\text{-}\alpha$ -hydroxylase appeared to be intact based on results from normal versus mutant mice that were all fed calcium and/or $1,25(\text{OH})_2\text{D}_3$ (59). However vitamin D and calcium deprived *Hyp* mice showed an abnormally high stimulation of $25(\text{OH})\text{D}_324\text{-}\alpha$ -hydroxylase (6 fold greater V_{max} than in normal mice treated the same way) when given $1,25(\text{OH})_2\text{D}_3$ or $1,25(\text{OH})_2\text{D}_3$ plus calcium (59).

(e) PTH response findings:

Parabiosis experiments on normal and *Hyp* mice have shown that the normal mice develop some of the features of hypophosphatemic rickets, namely hypophosphatemia and a decrease in renal Pi conservation (60). This finding supports the existence of a circulating

humoral factor as the cause of the disease. Even BBM vesicles isolated from normal mice joined to *Hyp* mice exhibited decreased Pi transport (60). Glucose transport was not inhibited in any way in these BBM vesicles, demonstrating the specificity of the transport defect induced by the union with the mutant animal (60). The possibility of PTH being this humoral factor was investigated since mutant mice are known to have secondary hyperparathyroidism. However, the phenotypic changes in the normal mouse were present even after parathyroidectomy (60). Although the study suggests that a humoral factor may be responsible for the disease state, PTH was not found to be this elusive humoral component.

(f) Protein kinase findings:

Based on findings that cAMP could mimic the effects of PTH on both the 25(OH)D₃1- α - and the 24- α -hydroxylases, Mandla et al. (61) postulated that the activation of cAMP-dependent protein kinase (PKA) was involved in regulation of vitamin D metabolism. However a direct correlation between the two has not been found. Also, PKA activity does not appear to be different in the *Hyp* mouse compared to the normal mouse. Thus the role of Ca⁺²-activated, phospholipid-dependent protein kinase (PKC), in the regulation of vitamin D metabolism, has been explored. Phorbol 12-myristate 13-acetate (PMA), a potent activator of PKC, was used to study 25(OH)D₃24- α -hydroxylase activity. PMA was unable to stimulate the already high 25(OH)D₃24- α -hydroxylase activity in mutant mice. However, use of a PKC inhibitor, H-7, abolished enzyme activity in both the normal and the mutant mouse (61). 25(OH)D₃24- α -hydroxylase activity can also be induced by supplementing the diet with 1,25(OH)₂D₃. H-7 was unable to inhibit this induced enzyme activity (61). The data suggested that PKC was involved in the regulation of constitutive but not 1,25(OH)₂D₃ inducible 25(OH)D₃24- α -hydroxylase and that PKC contributed to the abnormal expression of the 25(OH)D₃24- α -

hydroxylase enzyme activity in the hypophosphatemic mouse (61). Stimulation of PKC in normal mice lead to *Hyp* characteristics, namely deranged Pi transport in the kidney and vitamin metabolism (61). These findings further supported the notion that PKC was involved in the expression of the *Hyp* phenotype. Another study looked at the actual level of PKC found in the two genotypes whereas renal cytosolic PKC was found to be higher in *Hyp* mice than in normal mice, BBM and mitochondrial levels were similar in both strains (62). In order to really compare PKC levels, the PKC activity in Pi deprived normal mice was compared to the hypophosphatemic animals. Normal mice fed a Pi poor diet demonstrated no change in cytosolic PKC activity, a decrease in BBM PKC activity and an increase in mitochondrial PKC activity (62). For Pi deprived mutant mice there was no fall in the activity of PKC in the BBM. The stability of cytosolic PKC levels and the increase in mitochondrial PKC were identical in both Pi deprived genotypes. If the lack of Pi availability were a critical signal for the down regulation of PKC (demonstrated in Pi deprived normal mice), then the presence of normal levels of PKC activity BBM derived from *Hyp* mice, fed balanced or low Pi diets, implied that regulation of PKC may be abnormal in the *Hyp* kidney (62). In addition, since the greater activity of cytosolic PKC from mutant mice had been shown to be specific to the kidney it is possible that abnormal PKC activity may be related to the abnormal Pi transport and vitamin D metabolism that is characteristic of the *Hyp* mutation (62).

VIII. OBJECTIVES:

From the above presentation, it is evident that it is well established that XLH in humans and *Hyp* in mice are characterized by a derangement of Pi homeostasis at the level of the renal PCT. Compiled findings support the disruption of intracellular Pi balance which could lead to

abnormal cell response to external stimuli. Substantial data indicate that external stimuli sensed by cells are internalized by a series of events involving phosphatidylinositol 4,5-bisphosphate (PIP₂) metabolism and protein phosphorylation. The purpose of this study is to verify whether in the *Hyp* mouse there could be a defect in the second messenger pathway which could account for the wide variety of abnormalities outlined above. It has already been established that PKC levels are abnormally high in the *Hyp* mouse (62). Therefore our working hypothesis is that if inositol phosphate levels are also elevated then it is possible that the *Hyp* mouse possesses an abnormal guanyl nucleotide binding protein (G protein) since it is a common link between PKC and IP. We will verify how primary cultures of mouse kidney cells, from both normal and *Hyp* mice, are able to respond to 1,25(OH)₂D₃ and PTH in terms of inositol phosphate production, one aspect of the PKC activation pathway. A brief summary of the events involved in PIP₂ metabolism follows.

IX. PHOSPHATIDYLINOSITOL 4,5-BISPHOSPHATE METABOLISM:

It has been well established that PTH acts via coupling to adenylate cyclase, however other studies have shown PTH can increase intracellular Ca⁺² content in proximal tubule cells from mammalian kidney independent of cyclic nucleotides (63). Hruska et al. (63) demonstrated a PTH-dose dependent production of the second messengers 1,4,5-inositol phosphate (IP₃) and diacylglycerol (DAG) in opossum kidney cells, proximal tubule cells from primary culture and basolateral membranes from canine PT cells. This study concluded that PTH binds to a receptor at the cell surface and stimulates the hydrolysis of PIP₂ to yield IP₃ and DAG. PTH has also been found to elevate inositol phosphates and DAG in an osteoblast-like cell line stemming from the rat (64). It is likely that PTH carries out such an effect through

a membrane bound G protein coupled to phospholipase C (PLC) (64).

1,25(OH)₂D₃, like other steroid hormones, acts via its nuclear receptors to regulate the transcription of specific genes (65). However, rapid, non-genomic effects have also been noted for steroids. 1,25(OH)₂D₃ has been found to stimulate the PIP₂ pathway in enterocytes from 3 month old rats. As little as 5 seconds of exposure to 1,25(OH)₂D₃ was sufficient to see an increase in the levels of IP₃ and DAG accumulation (65). Therefore steroids are believed to bind to a cell surface receptor carrying out their effect within minutes, less time than necessary for protein synthesis as in the case of genomic effects (65-67).

As brief review, we must recall that the signal generated by extracellular 1,25(OH)₂D₃ must be converted to an intracellular one. Based on experiments showing rapid, non-genomic effects of this active form of vitamin D the second messenger system for this steroid hormone involves the activation of PLC (67). These results showed that 1,25(OH)₂D₃ required an intermediary to convey the message to its PLC effector. In general, the pattern followed for second messenger systems involves a G protein acting as a relay between an activated receptor and its effector (68). G proteins are made up of 3 unique subunits: α , β , and γ . The α subunit has been noted to be unique in all isolated G proteins, thus it is responsible for the G protein's specificity (69). However, the beta/gamma pair is not so diverse. In fact different α subunits have been found to be associated with the same $\beta\gamma$ subunit (69). The α subunit is believed to translocate within the membrane while the $\beta\gamma$ subunits remain together and are fixed in the membrane (69). The α subunit has a guanyl nucleotide binding site to which guanosine diphosphate (GDP) is bound when the receptor is unoccupied. Binding of an agonist induces conformational changes to the receptor allowing an interaction with the α subunit of the G protein, catalytic removal of GDP and its replacement with guanosine triphosphate (GTP) (69).

With GTP bound the G_{α} subunit dissociates from the $G_{\beta\gamma}$ subunit and activates the membrane bound PLC (69). PLC hydrolyzes the phosphodiester bond of PIP_2 , to yield IP_3 and DAG. The hydrolysis of GTP to GDP on the α subunit deactivates the G protein resulting in the dissociation of G_{α} from PLC and its reassociation with the $\beta\gamma$. Thus the G protein can regulate itself somewhat due to its GTPase activity. It should be noted that G-stimulatory (G_s) as well as G-inhibitory (G_i) proteins have been isolated (69). It is thought that the same $G_{\beta\gamma}$ subunits are able to associate with many G_{α} subunits, whether it be a G_i or G_s protein. Tying up the α subunit in such a way provides an additional regulatory mechanism. The cycling between the inactive trimeric form of the G protein and the active G_{α} with GTP bound to it is illustrated in figure 6.

This process of signal transduction allows for the amplification of a signal initiated by hormones or growth factors. A single ligand molecule binding to its receptor probably activates several G proteins simultaneously thus resulting in amplification of the signal (70). Such a system is of particular advantage when extracellular levels of ligands are low. Since several G proteins are activated, several PLC molecules catalyse the formation of IP_3 and DAG, yielding yet another step where amplification takes place (70). IP_3 's (phosphorylated at positions 1,4 and 5) half-life lasts only a few seconds. While biologically active, it rapidly diffuses to the endoplasmic reticulum (ER) and triggers release of Ca^{+2} into the cytoplasm (figure 7).

Binding of IP_3 to its intracellular receptor on the ER is yet another amplification step in the second messenger cascade (71). The release of intracellular Ca^{+2} also stimulates PLC thereby causing further hydrolysis of PIP_2 . IP_3 is metabolized by sequential dephosphorylation to IP_2 , IP and free inositol. The loss of the first phosphate at position 5 deactivates the IP_3 . IP_3 is also phosphorylated to 1,3,4,5- IP_4 which is then dephosphorylated to 1,3,5- IP_3 (71).

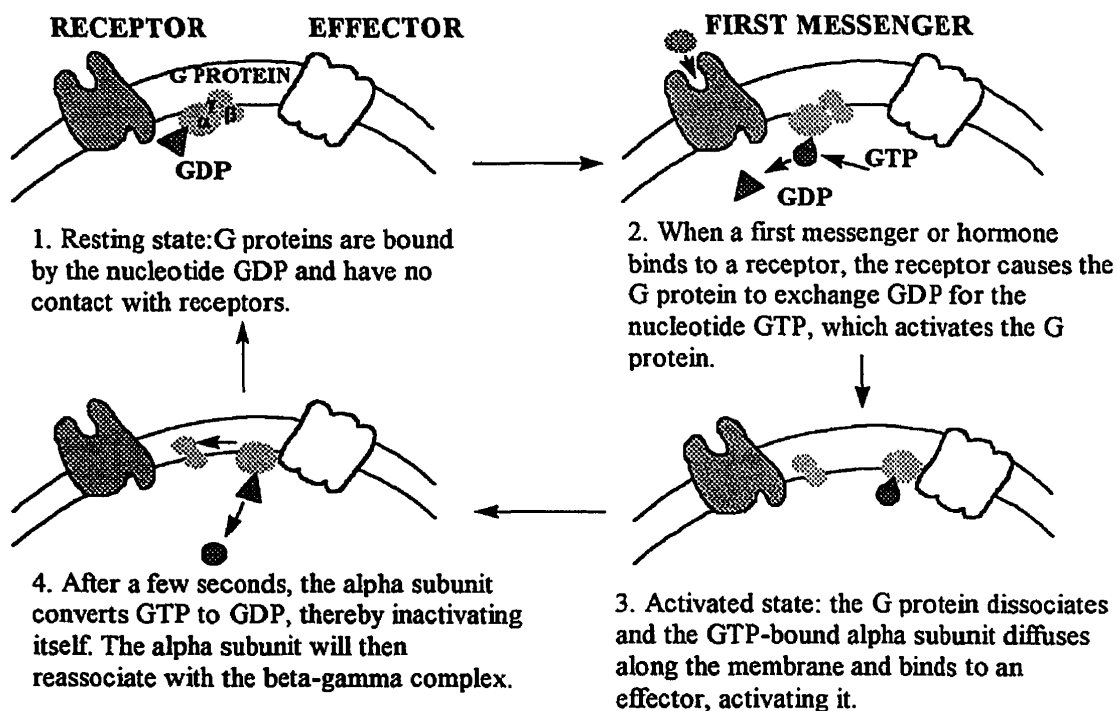


Figure 6. Summary of events in activation of G proteins as a result of ligand binding to its receptor (69).

DAG, the other second messenger generated by the hydrolysis of PIP_2 , is lipid soluble and membrane bound. Upon migration of PKC to the membrane, DAG activates the enzyme which in turn exerts its action by phosphorylating target proteins. DAG is metabolized to phosphatidic acid and then to cytosine diphosphate DAG which is recycled to the membrane in conjunction with inositol to form PIP_2 (71).

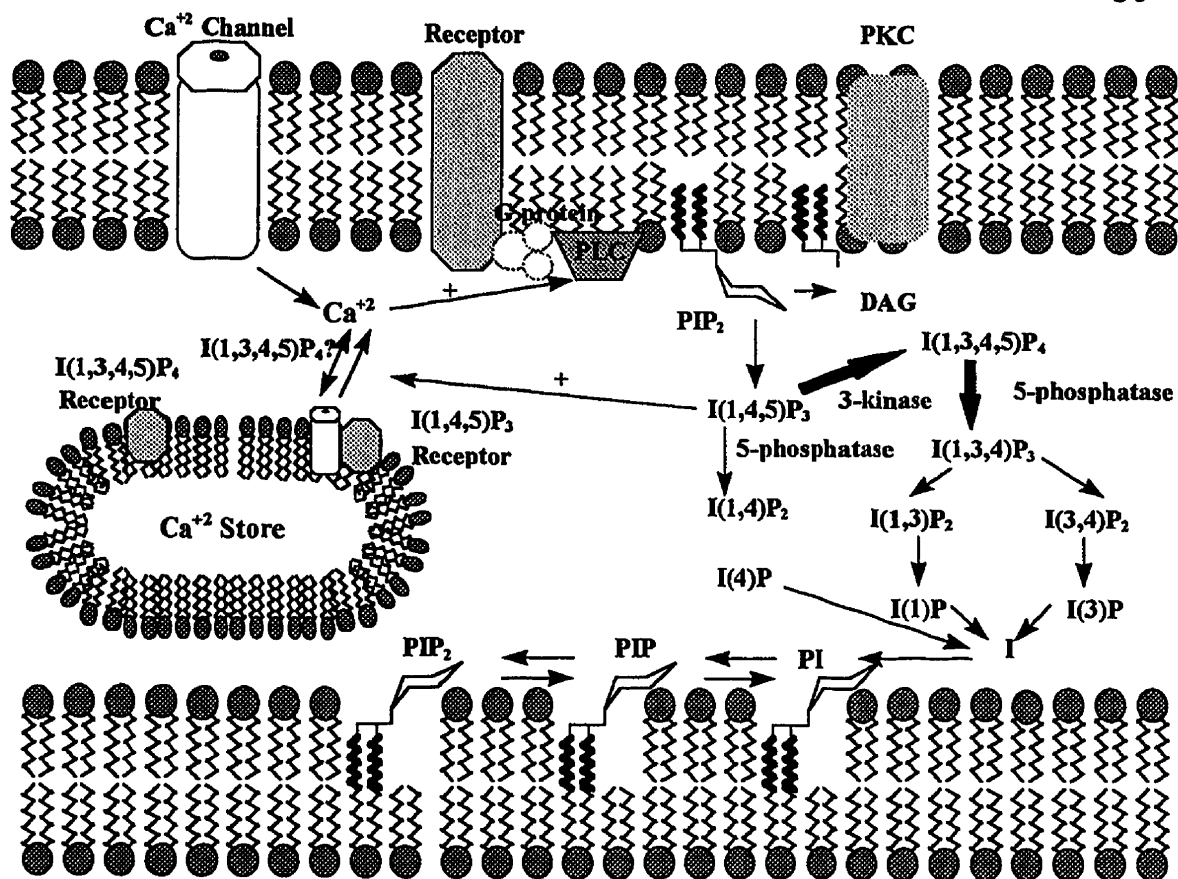


Figure 7. Schematic diagram of agonist stimulated inositol phosphate cascade (71).

MATERIALS

DMEM-F12, fetal calf serum and penicillin (5000 units/ml) streptomycin (5000 µg/ml) were obtained from Gibco. Insulin-transferrin-sodium selenite (ITS: 25mg, 25mg and 25 µg, respectively) and PTH (fragment 1-34) were purchased from Sigma Chemical Company (Oakville, Ontario). Collagenase A (from *Clostridium histolyticum*) was bought from Boehringer Mannheim (Laval, Quebec). Methanol, chloroform, hydrochloric acid, ammonium formate, disodium tetraborate and formic acid were purchased from BDH Inc. (St. Laurent, Quebec). Polyprep chromatography columns and AG 1X-8 ion exchange resin were bought from Bio-Rad Laboratories Inc. (Mississauga, Ontario). 1,25(OH)₂D₃ was kindly donated by Dr. M. Uskokovic from Hoffman LaRoche (Nutley, NJ). [³H] myo-inositol was purchased from Amersham. Cell culture dishes Falcon 3046 were obtained from Becton Dickson (Mississauga, Ontario). 100µm nylon mesh was obtained from B & SH Thompson & Co. The liquid scintillation counter used was a Packard 1600CA with Ecolite (ICN Biomedicals, Mississauga, Ontario) used as a scintillant.

Mice were bred in the animal facilities of the Genetics Unit of the Shriner's Hospital and maintained on a Purina Laboratory Chow (Ralston Purina of Canada Ltd., Montréal, Québec) containing 0.5% calcium and 0.74% phosphate. *Hyp*⁺ were crossed with +/Y and only male offspring were used to ensure the presence of the mutation. Inbred *Hyp* mice were initially provided by Dr. E. Eicher (Jackson Laboratory, Bar Harbor, ME). For +/+ bred with +/Y, only male offspring were used as well.

METHODS

(a) Renal cell culture:

Enriched primary cultures of proximal tubule cells were initiated from kidneys of 30 to 50 +/Y or *Hyp*/Y mice aged between 30 to 40 days. In order to try to reduce variability between cultures, normal and hypophosphatemic cultures were isolated on the same day as frequently as possible. The mice were anesthetized with ether and then decapitated. Kidneys were removed and placed in ice cold FMEM-F12 media (serum free). They were decapsulated and sliced longitudinally with a surgical blade. The medulla was sliced away, the remaining cortices were minced with a fresh, sterile surgical blade, placed in medium with 1 mg/ml of *Clostridium histolyticum* collagenase and incubated for 45 minutes at 37°C in a shaking waterbath. The suspension was subsequently filtered through a 100 µm nylon mesh to remove debris. The tissue remaining on the filter was washed twice with ice cold media. The cell suspension was centrifuged for 15 minutes at 800 rpm. The supernatant was discarded and the pellet was resuspended in ice cold media. This resuspension step was found to help in having less blood cells in the final culture. The suspension was once again centrifuged under the same conditions. The supernatant was discarded once again and the pellet resuspended in DMEM-F12 medium supplemented with 10% fetal calf serum. Cells were seeded in 35 mm Falcon tissue culture dishes such that one well served as the control and the remaining five were quintuplicates of the same stimulation. Twenty-four hours after plating the medium was replaced with DMEM-F12 medium supplemented with insulin (5 µg/ml), transferrin (5 µg/ml) and selenium (5nm/ml). Culture media was changed every other day. Cells were grown to confluency (usually 5 days from initial plating) in a humidified 5% CO₂/95% air incubator at 37 °C.

(b) Analysis of inositol phosphates:

Confluent cultures were given fresh media supplemented with 5 μ Ci of [³H]myoinositol. Cells were returned to the incubator for an additional 48 hours without medium changes. LiCl (10mM) was added for the last 2 hours of incubation to inhibit phosphatases. Cells were then challenged with 1-34 PTH at concentrations of 10⁻⁹ M to 10⁻⁷ M, 1,25(OH)₂D₃ at concentrations of 10⁻¹² M to 10⁻¹⁰ M for 1 minute in 5 μ l ethanol or the vehicle alone.

To stop the stimulation, media were aspirated and 1 ml of ice cold methanol containing 10 μ M phytic acid (inositol hexaphosphate) was added. Cells were scraped with a cell scraper and the lysed cells were transferred to extraction tubes. Extraction was performed according to the method of Bligh and Dyer with some modifications (72). In brief, 2.5 ml of a 1:2 chloroform/methanol mixture were added to the extraction tube. After vortexing and centrifuging (15 minutes at 2000 rpm) the aqueous phase was removed and set aside. The remaining lipid phase was washed with 2.5 ml of methanol/0.2 N HCl (1:1). After vortexing and centrifuging once again, the aqueous phase was combined with the first aqueous sample isolated above. The lipid phase was discarded. The combined aqueous samples were kept and chromatographed on a 1 ml column packed with Bio-Rad AG 1X-8 resin. Columns were prepared by washing with 10 ml H₂O, followed by 10 ml of 3M HCl and finally with 10 ml of ammonium formate. The aqueous sample was applied to the column followed by 10 ml of H₂O. The column was washed with 10 ml of 5 mM disodium tetraborate/60mM sodium formate, then with 10 ml of 0.2M ammonium formate/0.1 M formic acid, followed by 10 ml of 0.4M ammonium formate/0.1M formic acid and finally 1.0M ammonium formate/0.1M formic acid. Thus a total of 5 eluates were collected per applied sample. Half of each eluate was then counted in a Packard LS-6000 counter using Aquasol as a scintillant. The resulting counts

were then doubled to account for the entire 10 ml sample. Counts for IP_2 and IP_3 were very low and thus even the smallest fluctuations of results changed the mean significantly. Therefore the focus of this work is on the IP fraction. Percent incorporation was calculated as 'DPM for the IP eluate/total DPM collected for all 5 eluates'.

RESULTS

In order to show that the method of isolating proximal tubule cells did indeed yield PT enriched cultures, the proximal tubule enriched preparation was analyzed and verified in several ways.

(a) Morphology of confluent cells:

The morphology of the primary culture was verified at confluency by microscope. The cell monolayer exhibited epithelial shape and numerous domes characteristics of transporting epithelial cells as reported earlier (73).

(b) Metabolism:

Since the kidney PT is the known site of action of the 25(OH)D₃1- α - and the 24- α -hydroxylases, we verified that the isolated PT cells had retained their metabolic behaviour. Thus, enriched PT cultures from both normal and *Hyp* mice were incubated with [³H]-25(OH)D₃ for one hour. After extraction with diethylether, the labelled metabolites were separated by high performance liquid chromatography (HPLC). The products obtained were 25(OH)D₃, 24,25(OH)₂D₃, 25,26(OH)₂D₃ and 1,25(OH)₂D₃ (see figure 8). These products confirmed that the isolated cultures were PT enriched and that they retained their ability to metabolize the vitamin D precursor, 25(OH)D₃. In addition, as discussed, the *Hyp* mouse is expected to produce more 24,25(OH)₂D₃ than the normal mouse. This result was also observed for PT enriched cultures with *Hyp* cultures yielding six times as much 24,25(OH)₂D₃ than cells from normal mice.

(c) PIP₂ Metabolism:

After confirming that the primary culture is composed of a PT enriched cell population, the chromatography for separation of different IPs was standardized. The AG 1X-8 exchange resin columns were loaded with [³H] myo-inositol, [³H] inositol-4-phosphate, [³H] inositol-1,3-phosphate and [³H] inositol-1,3,5-phosphate.

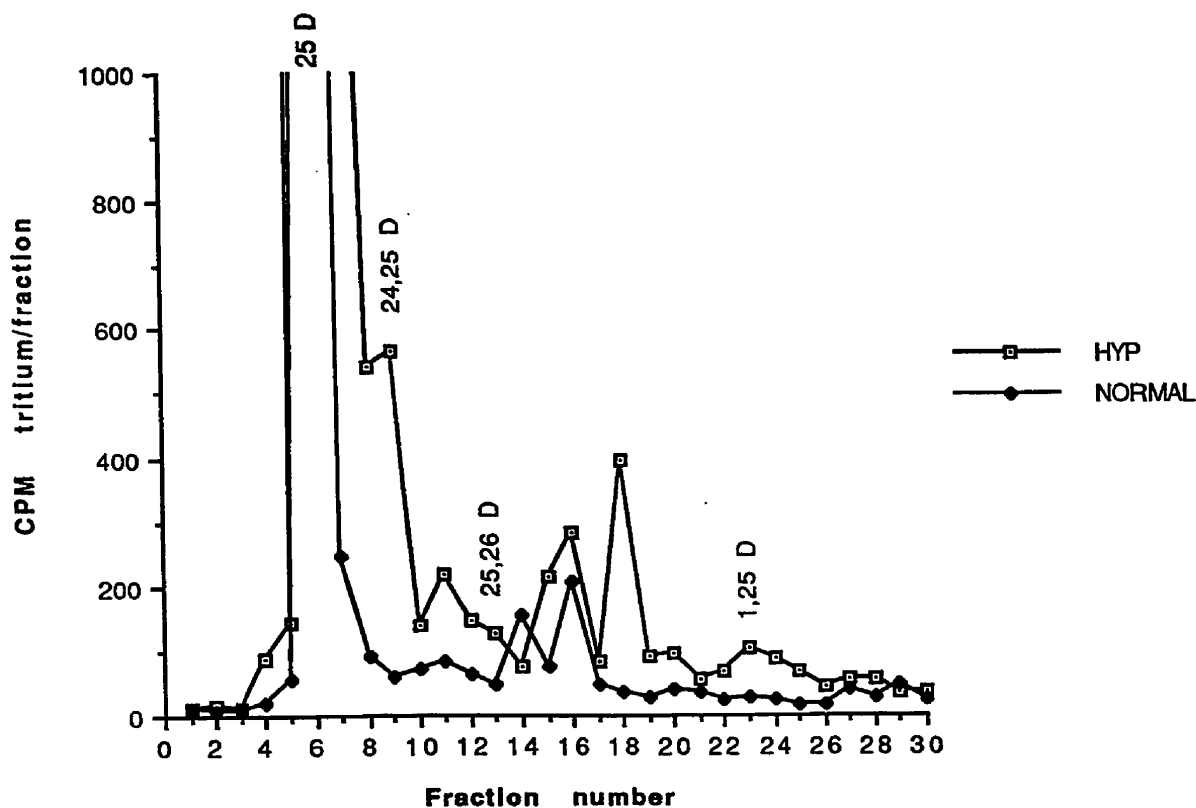


Figure 8. 25(OH)vitamin D₃ metabolism by PT enriched cultures from normal and *Hyp* mice.

The sequential elution of these standards with buffers of increasing ammonium formate and formic acid concentrations, showed a clear separation of each of all inositol compounds. No cross contamination was apparent among the different fractions. In addition the overall recovery of the labelled material was greater than 95%. Thus the assay system was determined to be suitable for the separation and study of the relative amounts of inositol phosphates produced.

Subsequently, normal PT enriched cultures were incubated with [^3H]myo-inositol for 48 hours in order to see if incorporation into inositol phosphates occurred. The total amount of incorporation was found to be approximately 8% as illustrated in figure 9 (incorporation into cyclic inositol phosphate fraction not shown). Four distinct labelled products were obtained. Free [^3H]myo-inositol is eluted first from the column with the four subsequent washes eluting cyclic inositol phosphates, IP, IP₂ and IP₃, respectively. The *Hyp* cultures were treated in the same manner and identical incorporation was noted. Therefore the pools of inositol phosphates are identical for the two genotypes. One limitation to the above method is, for example, the inability to separate the various isomers of IP₃. HPLC would have to be used to differentiate between the isomers.

(d) Analysis of inositol phosphates:

With the verification of both the cell culture method as well as the IP analysis method, it was then possible to investigate the metabolism of PIP₂ in PT cultures from normal and *Hyp* mice.

Based on previous experiments, a time course of 1 minute was found to be optimal for stimulation of PT cells. For cells isolated from +/Y mice a maximum stimulation for IP was

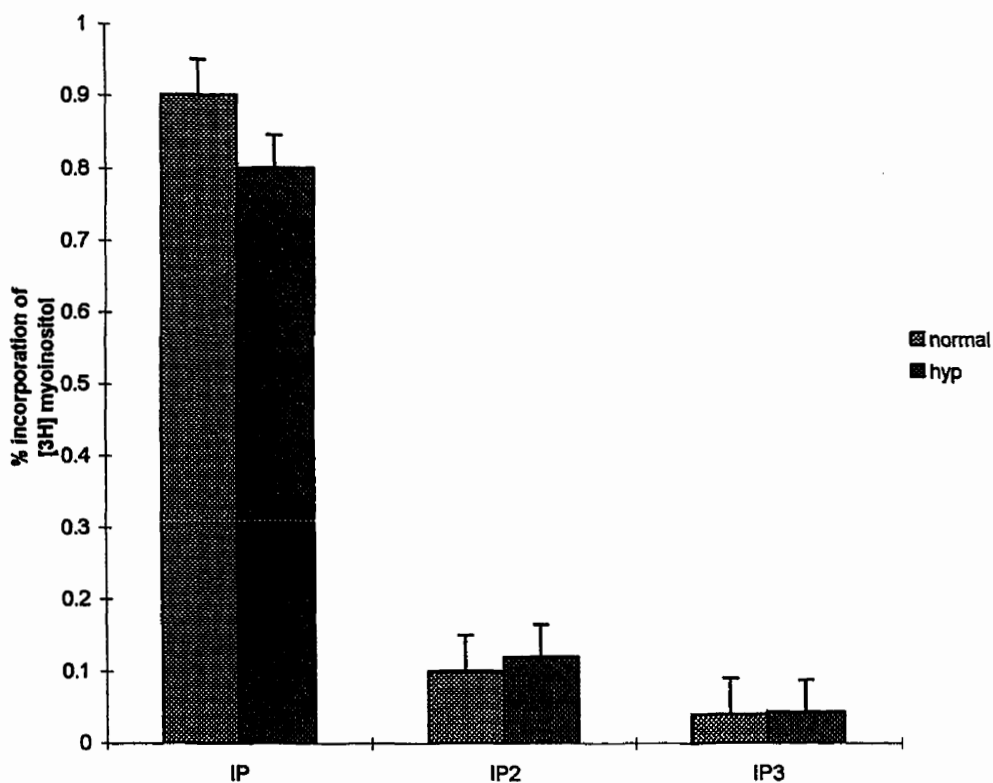


Figure 9. Total pools of [^3H] myo-inositol labelled products from PT enriched cultures from normal and *Hyp* mice (incorporation into cyclic inositol phosphate not shown).

observed at a concentration of 10^{-11}M $1,25(\text{OH})_2\text{D}_3$ ($1.548 \pm 0.631\%$, $p < 0.05$ compared to normal control). On the other hand the maximal IP response for *Hyp* PT cells was seen at 10^{-12}M $1,25(\text{OH})_2\text{D}_3$ ($1.628 \pm 0.638\%$, $p < 0.05$ compared to the *Hyp* control). Although the PT enriched cell cultures from normal and *Hyp* mice show different dose-response profiles, both appear to be stimulated to the same degree, with the mutant mouse being more sensitive to

1,25(OH)₂D₃. All results and statistics are found in table 2 and figure 10.

Group	IP ± S.D.	IP ₂ ± S.D.	IP ₃ ± S.D.
N control	0.631 ± 0.037	0.063 ± 0.007	0.024 ± 0.004
N 10 ⁻¹² M	1.272*# ± 0.046	0.082 ± 0.016	0.038 ± 0.008
N 10 ⁻¹¹ M	1.548*° ± 0.094	0.086 ± 0.014	0.038 ± 0.013
N 10 ⁻¹⁰ M	1.138*" ± 0.051	0.068 ± 0.015	0.028 ± 0.005
H control	0.638 ± 0.056	0.063 ± 0.008	0.024 ± 0.007
H 10 ⁻¹² M	1.628*() ± 0.052	0.101 ± 0.018	0.033 ± 0.006
H 10 ⁻¹¹ M	1.447*! ± 0.128	0.068 ± 0.014	0.024 ± 0.006
H 10 ⁻¹⁰ M	1.166* ± 0.080	0.068 ± 0.014	0.022 ± 0.005

n=25 N=normal H=*Hyp*

Values are the mean ± S.D. % incorporation of [³H] myo-inositol into IP, IP₂ and IP₃. Statistical significance was assessed by Anova/Fisher PLSD.

A difference between control and stimulated cultures with a p<0.05 was considered statistically significant.

* compared to N control and H control .

compared to N 10⁻¹¹M, N 10⁻¹⁰M, H 10⁻¹²M, H 10⁻¹¹M and H 10⁻¹⁰M.

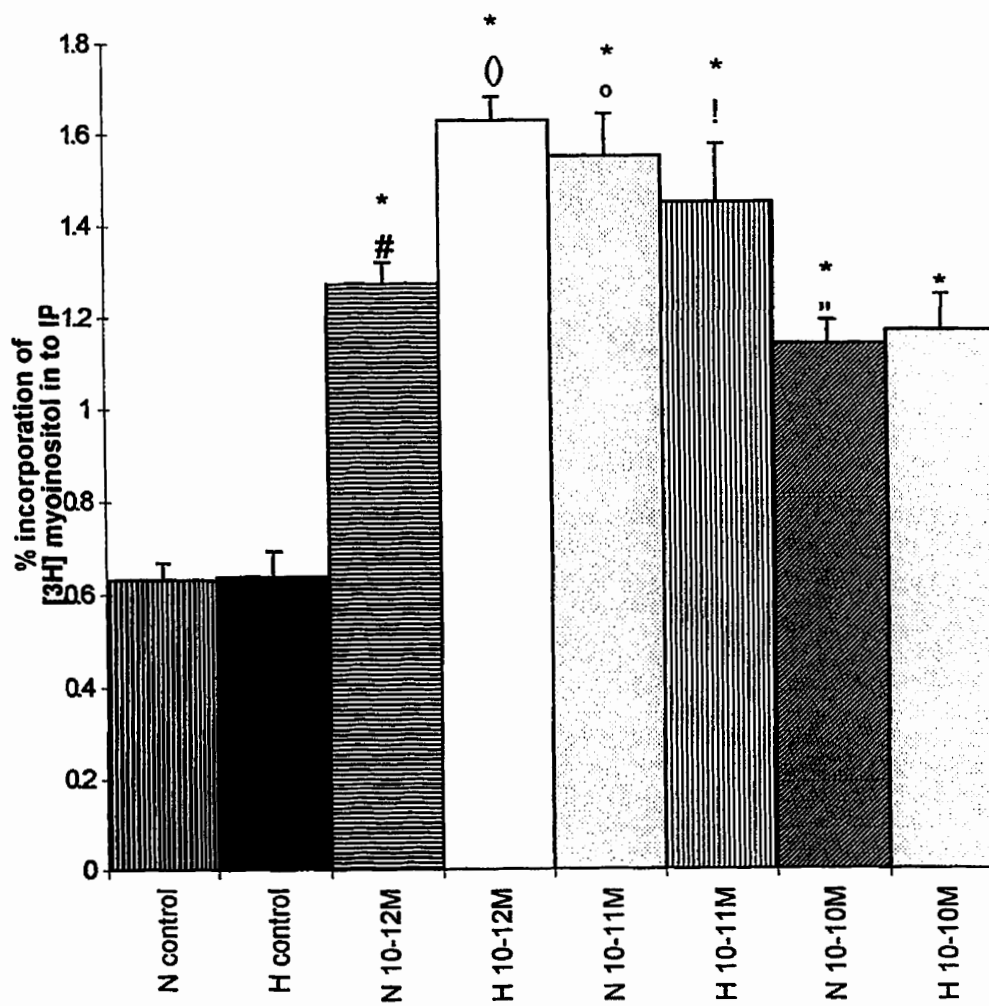
° compared to N 10⁻¹⁰M, H 10⁻¹²M, H 10⁻¹¹M and H 10⁻¹⁰M.

" compared to H 10⁻¹²M and H 10⁻¹¹ M.

() compared to H 10⁻¹¹M and H 10⁻¹⁰M.

! compared to H 10⁻¹⁰M.

Table 2. Percent incorporation of [³H] myo-inositol into inositol phosphate pools from PT enriched cultures stimulated with 1,25(OH)₂D₃ for 1 minute.



N = normal
H = *Hyp*

Figure 10. Percent incorporation of [^3H] myo-inositol into IP in PT enriched cultured stimulated with $1,25(\text{OH})_2\text{D}_3$ for one minute.

The same studies as above were repeated with PTH. We confirmed that PTH was able to stimulate the cleavage of PIP₂. In the case of PTH, the maximum responses for the wildtype and the mutant mice were in terms of magnitude, identical (10⁻⁸M) for the IP fraction (1.767 ± 0.037 % and 1.782 ± 0.063% incorporation, respectively, p>0.05). Furthermore, dose-response differences were evident between cultures of the genotypes. All data are summarized in table 3 with IP results illustrated in figure 11.

Group	IP ± S.D.	IP ₂ ± S.D.	IP ₃ ± S.D.
N control	0.596 ± 0.039	0.077 ± 0.017	0.050 ± 0.074
N 10 ⁻⁹ M	1.559*# ± 0.073	0.086 ± 0.016	0.035 ± 0.007
N 10 ⁻⁸ M	1.767*° ± 0.037	0.089 ± 0.016	0.042 ± 0.014
N 10 ⁻⁷ M	1.164** ± 0.057	0.088 ± 0.014	0.038 ± 0.008
H control	0.610 ± 0.042	0.078 ± 0.022	0.028 ± 0.011
H 10 ⁻⁹ M	1.576*() ± 0.051	0.087 ± 0.027	0.030 ± 0.013
H 10 ⁻⁸ M	1.782*! ± 0.063	0.084 ± 0.023	0.030 ± 0.014
H 10 ⁻⁷ M	1.213* ± 0.040	0.094 ± 0.032	0.031 ± 0.011

n=25 N=normal H=Hyp

Values are the mean ± S.D. % incorporation of [³H] myo-inositol into IP, IP₂ and IP₃. Statistical significance was assessed by Anova/Fisher PLSD.

A difference between control and stimulated cultures with a p<0.05 was considered statistically significant.

* compared to N control and H control.

compared to N 10⁻⁸M, N 10⁻⁷M, H 10⁻⁸M and H 10⁻⁷M.

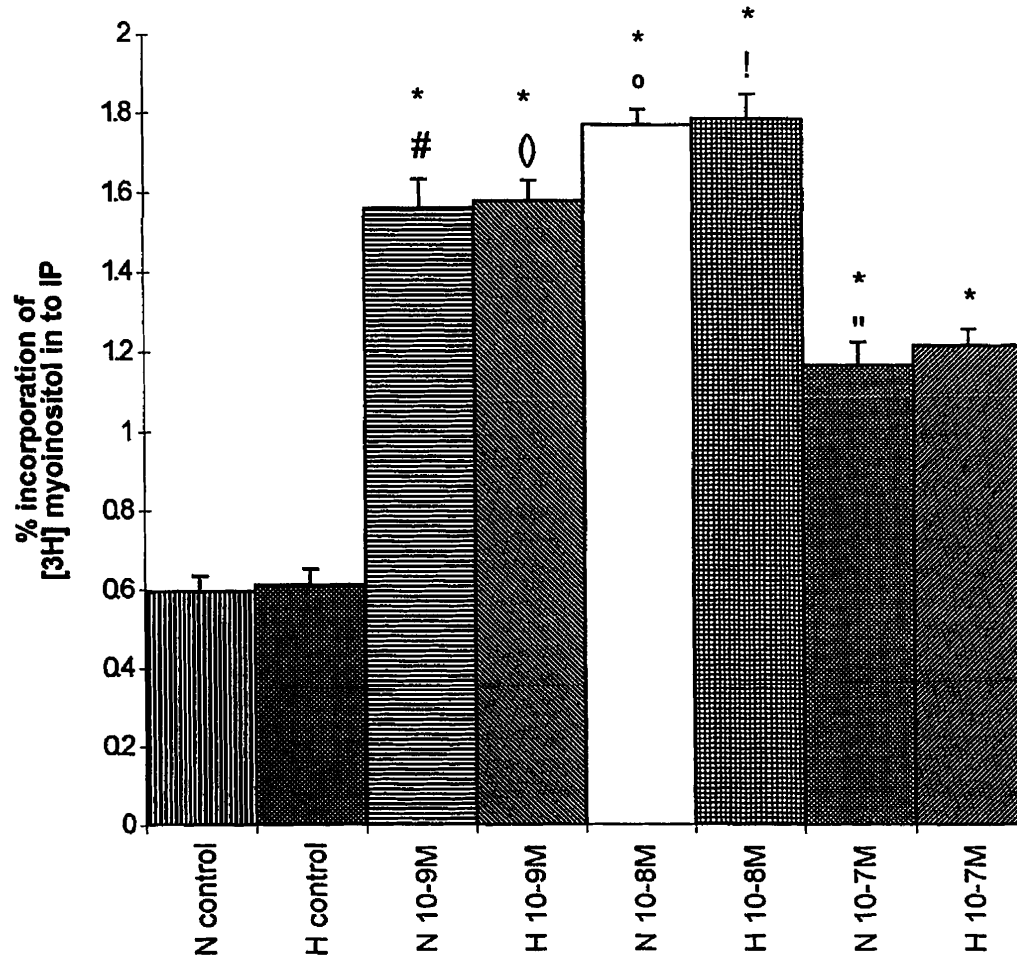
° compared to N 10⁻⁷M, H 10⁻⁹M and H 10⁻⁷M.

" compared to H 10⁻⁹M, H 10⁻⁸M and H 10⁻⁷M.

() compared to H 10⁻⁸M and H 10⁻⁷M.

! compared to H 10⁻⁷M.

Table 3. Percent incorporation of [³H] myo-inositol into inositol phosphate pools from PT enriched cultures stimulated with PTH for 1 minute.



N = normal

H = *Hyp*

Figure 11. Percent incorporation of [³H] myo-inositol into IP in PT enriched cultured stimulated with PTH for one minute.

Pertussis Toxin (PTX) catalyzes the ADP-ribosylation of a cysteine residue in the α subunit of Gi proteins activating the PIP₂ signalling pathway (74). We therefore designed a series of experiments to test whether PCT enriched cultures from *Hyp* mice responded differently to the toxin than do the cultures from +/Y animals. PCT preparations were cultured as discussed in the Method Section. At confluency, normal and *Hyp* PT enriched cultures were stimulated with PTX with or without 10⁻¹¹M 1,25(OH)₂D₃. This experiment demonstrated that the *Hyp* PT cells were insensitive to the toxin (0.937 ± 0.054%, p>0.05 compared to *Hyp* control cultures). Normal cells challenged with 1,25(OH)₂D₃ alone compared to normal cells given PTX alone showed no difference between IP fractions (1.576 ± 0.145% and 1.581 ± 0.168% respectively, p>0.05). *Hyp* cells on the other hand gave rise to 1.497 ± 0.110% incorporation into IP fractions when given 1,25(OH)₂D₃, compared to only 0.937 ± 0.054% for *Hyp* PT cells exposed to PTX alone (p<0.05). *Hyp* PT cells did also exhibit a response above that of PTX alone when challenged with PTX and 1,25(OH)₂D₃ together (1.284 ± 0.365% incorporation, p<0.05). The above results are summarized in table 4 and figure 12.

The same results were obtained when the above experiments were repeated using PTH as a stimulant in presence of PTX. Normal cells showed no difference in stimulation when challenged with PTH alone, PTX alone or PTX plus PTH (1.528 ± 0.052%, 1.581 ± 0.168% and 1.560 ± 0.221% incorporation, respectively, p>0.05). *Hyp* cells showed no stimulation with PTX but did produce a response when given PTH and PTH plus PTX (0.937 ± 0.054%, 1.377 ± 0.080% and 1.251 ± 0.151% incorporation, respectively, p<0.05 for PTH versus PTX only). All results are presented in table 5 and figure 13.

Group	IP \pm S.D.
N control	1.036 \pm 0.182
N 1,25(OH) ₂ D ₃	1.576*# \pm 0.145
N PTX	1.581*# \pm 0.168
N 1,25(OH) ₂ D ₃ /PTX	1.651*# \pm 0.236
H control	0.892 \pm 0.070
H 1,25(OH) ₂ D ₃	1.497*() \pm 0.110
H PTX	0.937! \pm 0.054
H 1,25(OH) ₂ D ₃ /PTX	1.284* \pm 0.365

n=5 N=normal H=Hyp 1,25(OH)₂D₃= 10-11M
 PTX= 100 ng/ml Pertussis Toxin

Values are the mean \pm S.D. % incorporation of [³H] myo-inositol in to IP, IP₂ and IP₃.

Statistical significance was assessed by Anova/Fisher PLSD.

A difference between control and stimulated cultures with a p<0.05 was considered statistically significant.

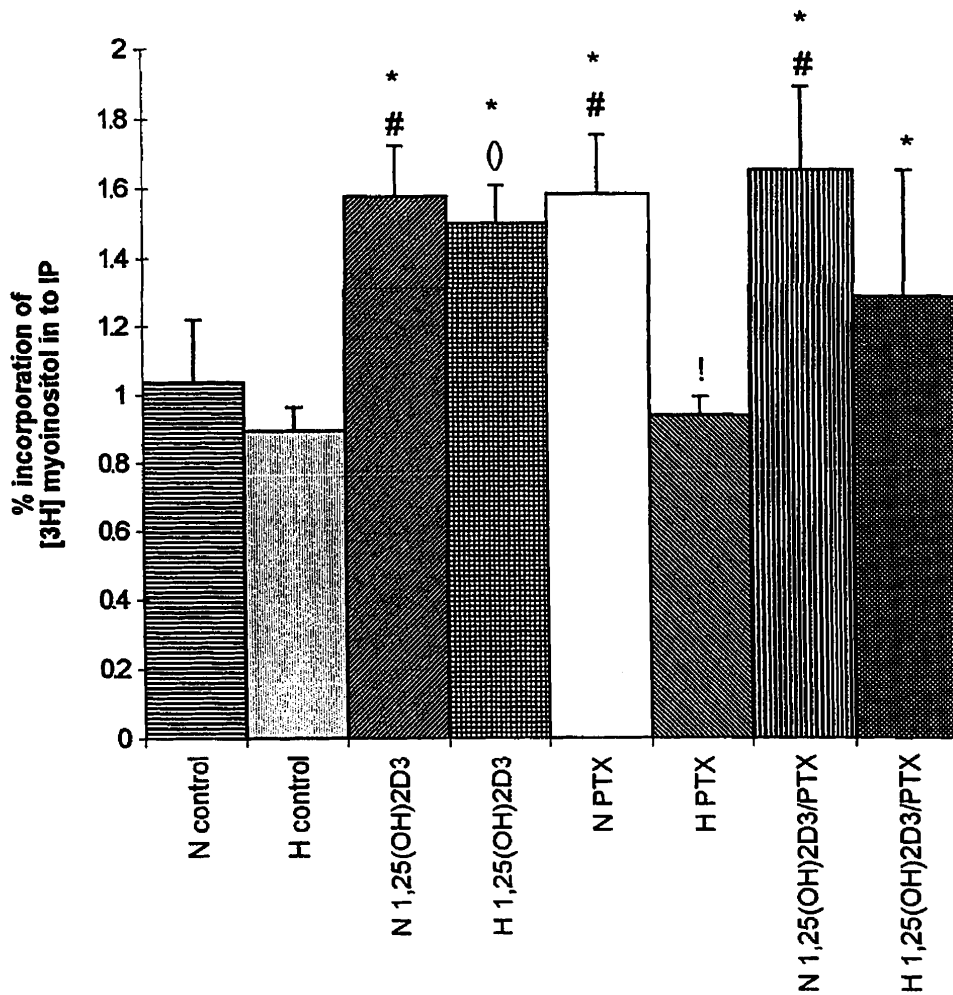
* compared to N control and H control.

compared to H PTX and H 1,25(OH)₂D₃/PTX.

() compared to H PTX.

! compared to H 1,25(OH)₂D₃/PTX.

Table 4. Percent incorporation of [³H] myo-inositol into inositol phosphate pools from PT enriched cultures stimulated with 1,25(OH)₂D₃ for 1 minute with or without preincubation with PTX for 4 hours.



N = normal

H = *Hyp*

Figure 12. Percent incorporation of [³H]myo-inositol into IP in PT enriched cultures stimulated with 1,25(OH)₂D₃ for one minute with or without preincubation with 100 ng/ml PTX for 4 hours.

Group	IP \pm S.D.
N control	1.036 \pm 0.182
N PTH	1.528*# \pm 0.052
N PTX	1.581*° \pm 0.168
N PTH/PTX	1.560*° \pm 0.221
H control	0.892 \pm 0.070
H PTH	1.377** \pm 0.080
H PTX	0.937() \pm 0.054
H PTH/PTX	1.251* \pm 0.151

n=5 N=normal H=Hyp PTH= 10^{-9} M
 PTX= 100 ng/ml Pertussis Toxin

Values are the mean \pm S.D. % incorporation of [3 H] myo-inositol into IP, IP2 and IP3.

Statistical significance was assessed by Anova/Fisher PLSD.

A difference between control and stimulated cultures with a $p < 0.05$ was considered statistically significant.

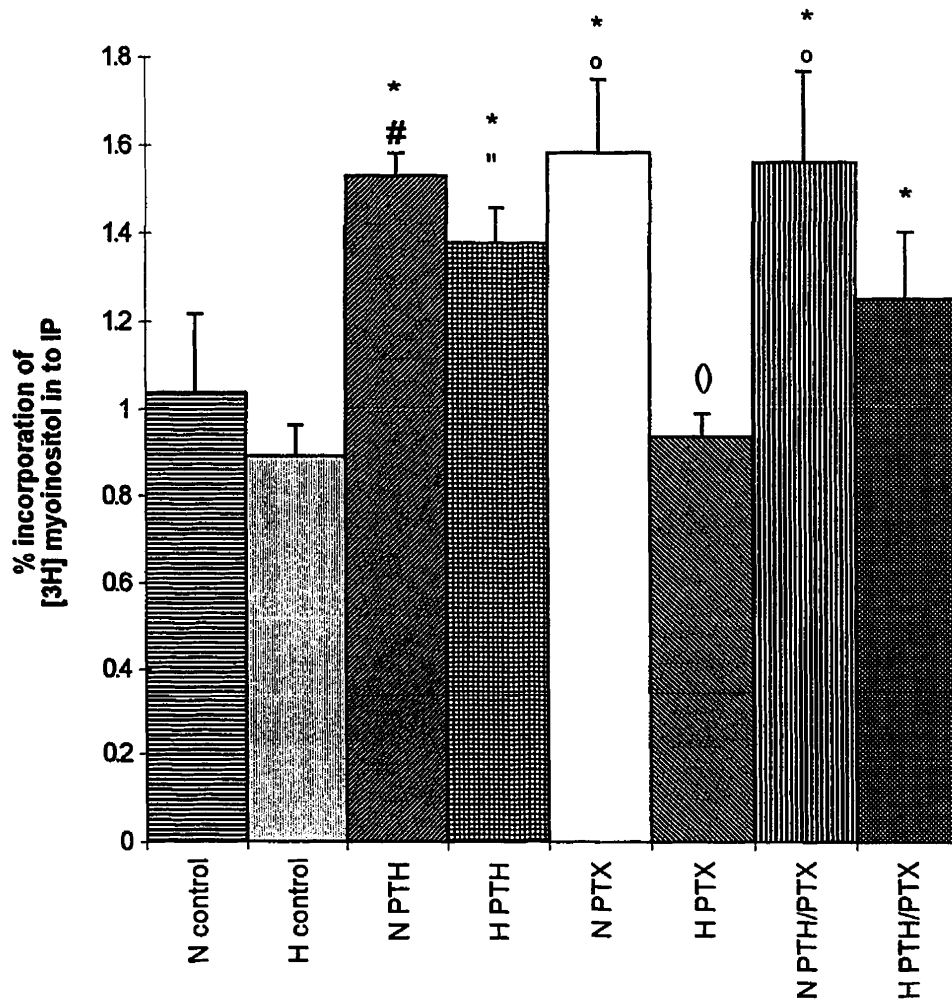
* compared to N control and H control.

compared to H PTX and H PTH/PTX.

° compared to H PTH, H PTX and H PTH/PTX.

() compared to H PTH/PTX.

Table 5. Percent incorporation of [3 H] myo-inositol into inositol phosphate pools from PT enriched cultures stimulated with PTH for 1 minute with or without preincubation with PTX for 4 hours.



N = normal
H = *Hyp*

Figure 13. Percent incorporation of [³H]myo-inositol into IP in PT enriched cultures stimulated with PTH for one minute with or without preincubation with 100 ng/ml PTX for 4 hours.

DISCUSSION

We have tested the hypothesis that PCT from *Hyp* mouse kidney respond differently to G protein agonists than those of the +/Y mouse, thereby suggesting a mechanism for the abnormally high PKC seen in *Hyp* mice (62).

We have shown that PT enriched cultures from normal mice, when stimulated with $1,25(\text{OH})_2\text{D}_3$ for one minute, produced a maximum generation of IP at 10^{-11}M . *Hyp* mice, on the other hand, exhibited a maximum response at 10^{-12}M . These two concentrations of $1,25(\text{OH})_2\text{D}_3$ are close to the physiological level of $1,25(\text{OH})_2\text{D}_3$, 10^{-10}M . This rapid response to the steroid hormone supports the previous studies showing that $1,25(\text{OH})_2\text{D}_3$ does have non-genomic effects (65, 67). *Hyp* PT cells exhibit a one order of magnitude increase in sensitivity to the hormone than normal PT cultures. Whether this observation supports the elevation in PKC activity seen in *Hyp* kidneys remains to be elucidated (62, 75). Our working hypothesis was also based on previous studies such as one by Wali et al. (76) focusing on rat colonic epithelium. This study demonstrated that $1,25(\text{OH})_2\text{D}_3$ caused a rapid decrease in colonic levels of membrane phosphoinositides and an increase in the cellular content of inositol phosphates (76). Stimulation was less sensitive than in our system, exhibiting maximal results at 10^{-8}M concentrations of $1,25(\text{OH})_2\text{D}_3$. The discrepancy in stimulation may arise from species and/or tissue differences in the models used. Increases in IP were seen as early as 15 seconds with the maximum being reached between 30 and 60 seconds, the same time frame as our results. This study also demonstrated that $1,25(\text{OH})_2\text{D}_3$ stimulated the formation of DAG and activated PKC which temporally coincides with DAG formation (76). The confirmation that IP_3 , DAG and PKC are all elevated in the study by Wali et al., supports the objectives of our

experiments, namely that we can correlate IP results with previous PKC findings. The combination of these two findings, elevated PKC levels and increased sensitivity to $1,25(\text{OH})_2\text{D}_3$ by *Hyp* PT cells suggest the presence of altered signalling in *Hyp* PT cells. The altered signal may stem from a G protein since it is such an activated G protein that leads to PIP_2 cleavage and subsequent PKC activation and IP_3 production.

Previous work on the action of $1,25(\text{OH})_2\text{D}_3$ on PIP_2 metabolism in rat enterocytes reported maximal IP production after a 30 second stimulation with 10^{-12}M $1,25(\text{OH})_2\text{D}_3$ (77). This study also found that the generation of IP was dose dependent and biphasic. These results correlate with what was found in PT cultures from normal and *Hyp* mice. The same dose response effect was observed as in our study and the maximal stimulation occurred in the same concentration range.

It is interesting to note that cAMP has commonly been accepted as the main intracellular mediator of PTH action in both osteoblasts and kidney cells (78, 79). Studies have however shown that PTH stimulates PIP_2 hydrolysis via PLC in renal tubular cells (80). A previous study on confluent opossum kidney cells with or without the PLC inhibitor, U-73-122, showed that the inhibitor did not affect cAMP production but did however eliminate PTH induced increases in diglyceride mass, indicating PLC inhibition (80). Since our model is also able to produce IP's in response to PTH, it contributes to the growing support that PTH acts not only via cAMP but also via PLC. In our studies, when using PTH as an agonist, both PT cultures from normal and *Hyp* mice were observed to yield a maximum IP response at 10^{-8}M . The identical response of both cultures demonstrates that the *Hyp* PT cells respond normally to PTH. This finding confirms that the increased sensitivity of *Hyp* mice to $1,25(\text{OH})_2\text{D}_3$ is a

specific one. Since PTH and $1,25(\text{OH})_2\text{D}_3$ more than likely act through different G proteins, the data may suggest an abnormality in the G protein coupled to the putative $1,25(\text{OH})_2\text{D}_3$ cell surface receptor in *Hyp* PT cells. The similarity of the PTH response in both sets of cultures correlates well with previous *in vivo* studies concluding that the kidneys of *Hyp* mice are not hypersensitive to exogenous PTH (81).

It should be mentioned that the physiological level of PTH normally seen is of the order of 10^{-14} M, compared to the range of concentrations for which we saw a dose-response relationship (10^{-9} M to 10^{-7} M). In our *in vitro* experiments, it is impossible to know how much of the PTH is actually reaching the cells. Rapid degradation of PTH may occur and therefore more PTH must be used in order to keep a certain amount available to the cells. Also we are working with concentrations to give a maximal response and depending upon the model used the concentration of PTH to obtain an optimal effect may differ. One previous study by Hruska et al. (82) demonstrated that PTH produced a dose dependent immediate stimulation of IP and DAG production in the opossum kidney cell line, primary culture PT cells and BLM from canine tubular segments, with the most significant results occurring in the opossum kidney cell line. Opossum kidney cells required a minimum of 10^{-10} M PTH with 10^{-7} M producing the maximum in a time frame of 30 seconds to 5 minutes. This concentration range is similar with ours, in both cases PTH had to be well above physiological levels to produce stimulation. Membrane preparations of canine renal cortical tubular cells needed an even greater amount of PTH for maximum stimulation of IP's, 10^{-6} M for 30 seconds (83). Investigation of PTH stimulation of IP metabolism in an osteoblast like cell line (UMR 10-01) showed maximal stimulation at 10^{-7} M in 30 to 60 seconds (84). All of the above studies indicate that our

maximum at 10^{-8} M PTH is an acceptable level, despite its deviation from the physiological.

In order to pursue the possibility of an altered membrane in the *Hyp* PT cells, PTX was incorporated into the experimental to investigate G proteins. Interestingly, normal PT cultures were able to hydrolyse PIP₂ in the presence of PTH, 1,25(OH)₂D₃ or PTX. It is also noteworthy that normal cultures showed no additive effect when challenged with PTX and agonist, either 1,25(OH)₂D₃ or PTH. The lack of an additive effect may indicate that pretreatment with PTX already causes maximum stimulation of the cells. Little data exist on PTX effects on G proteins coupled to PLC. One study of UMR 106-01 osteoblast like cells noted no effect of PTX pretreatment (500ng/ml for 6 hours) on 10^{-7} M PTH stimulation of IP formation (84). These results correlate with our observations that no additive effect was seen for PTH plus PTX. The study unfortunately fails to report if there is any IP production in response to PTX alone, thereby prohibiting further comparison. A lack of data in the literature, concerning 1,25(OH)₂D₃ and PTX effects, demonstrate the need for further studies in this area. Based on our results, it would be interesting to investigate PIP₂ hydrolysis using much lower concentrations of PTX and/or agonist. It may then be possible to detect an additive effect when using toxin and hormone.

On the other hand, in the *Hyp* PT cultures, PTH and 1,25(OH)₂D₃ stimulate PIP₂ hydrolysis while PTX has no effect. Despite the unresponsiveness of *Hyp* cultures to PTX, the cells were able to be stimulated in the presence of PTX with agonist. We may conclude from this that the tubules are for some reasons insensitive to the toxin. One possibility for the difference between normal and *Hyp* cultures would be that the G protein is altered in the mutant animal membrane. It would be interesting to perform the same experiments using

cholera toxin since this toxin is known to ADP-ribosylate G_s proteins. Therefore it may be possible to detect if more than one type of G protein is different in the *Hyp* mouse.

Having discussed our findings it is important to discuss the cell culture technique and the potential margins of error in this experimental model. Cultured cells may not express the phenotype of the tubules from which they were obtained since dedifferentiation may take place in culture to a certain extent thereby giving rise to the masking of the *Hyp* phenotype (43). Also there still remains the question of the purity of the primary culture. It is impossible to know how heterogeneous the cell population is. In particular it is improbable that the homogeneity of the culture is identical from one preparation to the next, thereby introducing a margin of error into the results. Also, the presence of contaminating DT cells which do not express the *Hyp* mutation, may mask the phenotype (43). It is important to note that the culturing of PT cells away from their usual environment introduces the advantage of removing them from humoral factors. Thus the increased sensitivity of *Hyp* cultures to $1,25(OH)_2D_3$ which we have found supports the notion of an intrinsic defect in PT cells and not an altered circulating, humoral factor.

For both $1,25(OH)_2D_3$ and PTH experiments, we have expressed the generation of IP as a percentage of the total radioactivity recovered. Thus we have eliminated the need to express our results in DPM, as others have done as well (67, 77). It is more difficult to analyse the IP_2 and IP_3 data. Since the actual number of DPM being generated for these two species is so low, any fluctuations in the counts leads to a large standard deviation. Attempts were made to try to improve the experimental protocol. Longer stimulation with the agonists was performed (fifteen minutes) in order to determine if an accumulation of the various inositol

phosphates would occur. However no improvement was detected nor was an accumulation of products seen (data not shown). Other attempts were also made to obtain higher values for IP₂ and IP₃. Recall the presence of LiCl during the last 2 hours of incubation prior to stimulating the cells. LiCl is present in order to inhibit the dephosphorylation of IP to free inositol. Several concentrations of LiCl were investigated, however no improvement was seen in the stability of IP₂ and IP₃ fractions when compared to the original protocol. Others have also reported that the presence of 10 mM LiCl still resulted in rapid dephosphorylation of IP to inositol (85). Thus, since the IP fractions gave reliable results, the data for IP₂ and IP₃ were not discussed.

The above results show that both 1,25(OH)₂D₃ and PTH stimulate the PIP₂ pathway in primary cultures of tubular cells, with *Hyp* mice exhibiting sensitivity to 1,25(OH)₂D₃. It would be relevant to verify that the increase in IP and DAG (or PKC) production is accompanied by a decrease in the PIP₂ level in the membrane. This procedure would also eliminate the need to study IP₂ and IP₃ individually. The decrease in PIP₂ would represent the generation of all inositol phosphates. Perhaps it would be possible to demonstrate a stoichiometric relationship between the increase in products and the decrease in the membrane phospholipid. For such experiments, the cell cultures would have to be labelled not only with [³H]myo-inositol, but also with [¹⁴C]-arachidonic acid or [¹⁴C]glycerol. Thus the lipid soluble fractions would also be radio labelled. The aqueous phase would be processed as described earlier. The lipid phase would be collected this time and analyzed by one dimension thin layer chromatography. After processing as described (86), the appropriate lipid of interest can be quantified by scintillation counting.

In addition to determining if PIP₂ decreases to the same degree as IP and DAG

increase, it would also be important to investigate the signalling pathway at the membrane level. As was mentioned earlier both PTX and cholera toxin are useful for this purpose. Also, non-hydrolyzable guanidyl phosphate analogues could be used to determine the role of the different G proteins likely to interact with the agonist/receptor complex. Such analogues are able to induce a sustained activation of the G protein and are therefore useful in enhancing the signals. This approach would enable us to test whether the signalling mechanisms (at the membrane level) responsible for the phosphorylation of endogenous proteins are affected by the *Hyp* mutation.

Stimulation of second messenger systems opens the way to the modulation of intracellular calcium. As was mentioned previously, increase of cellular IP_3 leads to the onset of a calcium signal. The measurement of such intracellular calcium levels can be performed on single cells. Cells can be grown on microscope slides for this purpose. The cells can then be exposed to agonist and incubated in presence of FURA-2 (87). The release of calcium can then be correlated to the amount of fluorescence detected. This calcium release would then be indicative of the extent of IP_3 production. Such protocol would eliminate some of the error introduced when using a different cell culture preparation for each experiment since many experiments can be conducted on the same cell. Also if the cell that is chosen is taken from a dome formation clearly visible by microscope, this method would also eliminate the possibility of contaminating DT cells. Data from both the second messenger pathway and the measurement of cytosolic calcium may shed light, at the cellular level, on the pathophysiology of the *Hyp* trait and thus on XLH.

Despite extensive biochemical studies of the *Hyp* mouse, the gap in information

stresses the need for techniques such as positional cloning which may provide greater insight in to the disease within a faster time frame than any of the areas described above. Positional cloning has the advantage of not being dependent on knowing gene function in order to locate the disease gene (36). Instead, this technique relies on initially determining the chromosomal localization of the gene and narrowing down the area by genetic linkage analysis (35). Already a detailed map of the *Hyp* region exists which has given rise to the discovery of PEX (phosphate regulating gene with homologies to endopeptidases, on the X chromosome) (37). Individuals with XLH have been observed to possess PEX deletions, splice shift and frameshift mutations which are the most probable cause of loss of function of the PEX gene product (37). It is however unknown at this point how PEX might regulate Pi homeostasis. The most likely function of PEX is that it is involved in processing of a hormone that directs Pi handling (37).

Du et al. (88) have recently cloned the murine *Pex* gene. This cDNA encodes the mouse counterpart of the human PEX gene. This mouse *Pex* cDNA encodes a predicted protein with 95% homology to the available human PEX sequence (88). Strom et al. (89) have shown that the 3' end of this gene is deleted in the *Hyp* mouse. Du et al. also demonstrated expression of the gene in bone but not in kidney, liver and intestine. It is suggested that a bone gene product may be part of a pathway that regulates renal phosphate homeostasis. The lack of expression in the mouse kidney supports the theory of a humoral factor. Identification of the role of *Pex* in phosphate homeostasis awaits the identification of this putative circulating factor. The advantage of the existence of a murine homologue to PEX are the ability to conduct expression studies and to search for modifier genes in the mouse (89). Future studies are necessary to first identify the normal function of the PEX gene product and the mechanism by

which its mutation leads to human and likely murine XLH (88).

CONCLUSION

Our results show that *Hyp* PCT from mouse have a higher sensitivity to $1,25(\text{OH})_2\text{D}_3$ than those from $+/\text{Y}$ mice. Furthermore they exhibit a difference in response to PTX. Both sets of results suggest that the membrane PLC system and G protein are somewhat modified in the *Hyp* phenotype. The results therefore support earlier observations which have shown an increase in PKC activity (62) and could be explained by the mutant PEX. This endopeptidase could modify G protein structure in the region where PTX is bound.

REFERENCES

1. Favus, M.J., ed. (1993): Primer on the Metabolic Bone Diseases and Disorders of Mineral Metabolism. 2nd edition, Raven Press, USA, 3-9, 15-40.
2. Ganong, W.F. (1991): Review of Medical Physiology. 15th edition, Appleton & Lange, Connecticut, USA, 292, 564 and 650.
3. Seldin, D.W. and Giebish, G., eds (1992): The Kidney: Physiology and Pathophysiology. 2nd edition, Raven Press, USA, v.1-v.3, 54.
4. DeGroot, L.J. (1979): Endocrinology. Grune and Stratton, New York, vol.2, 559-570.
5. Scriver, C.R. ed. (1995): The Metabolic Basis of Inherited Disease. 7th edition, McGraw-Hill Inc., USA, 3717-3745.
6. Walling, M.W. (1977): Intestinal Ca and Phosphate Transport: Differential Responses to Vitamin D₃ Metabolites. *Am J Physiol* 233:E488-494.
7. Guyton, A.C. (1996): Textbook of Medical Physiology. 9th edition, W.B. Saunders & Co., USA, 937-951.
8. Vander, A.J., ed. (1985): Renal Physiology. 3rd edition, McGraw Hill Book Co., NY, USA, 6-17.
9. Massry, S.G. and Fleisch, H. (1980): Renal Handling of Phosphate. Plenum Publishing Co., N.Y., 78-79.
10. Gmaj, P. and Murer, H. (1986): Cellular Mechanisms of Inorganic Phosphate Transport in Kidney. *Physiol Rev* 66: 36-70.
11. Dennis, V.W. et al. (1977): Response of Phosphate Transport to Parathyroid Hormone in Segments of Rabbit Nephron. *Am J Physiol* 233:F29-38.
12. Freeman, D et al. (1983): Energetics of Sodium Transport in the Kidney Saturation Transfer ³¹P NMR. *Biochim Biophys Acta* 762: 325-336.
13. Baylink, D. et al. (1971): Formation, Mineralization and Resorption of Bone in Hypophosphatemic Rats. *J Clin Invest* 50: 2519-2530.
14. Murer, H. and Burckhardt, G. (1983): Membrane Transport of Anions Across Epithelia of Mammalian Small Intestine and Kidney Proximal Tubule. *Rev Physiol Biochem Pharmacol* 96: 1-51.

15. Quamme, G.A. et al. (1985): Effects of Intraluminal pH and Dietary Phosphate on Phosphate Transport in the Proximal Convoluted Tubule. *Am J Physiol* **249**: F759-768.
16. Kempson, S.A. and Dousa, T.P., (1979): Phosphate Transport Across Renal Cortical Brush Border Membrane Vesicles from Rats Stabilized on a Normal, High or Low Phosphate Diet. *Life Sc* **24**: 881-888.
17. Nakagawa, N. et al. (1991): Characterization of the Defect in the Na⁺-Phosphate Transporter in Vitamin D-resistant Hypophosphatemic Mice. *J Biol Chem* **266**: 13616-13620.
18. Beliveau, R. and Brunette, M.G. (1984): The Renal Brush Border Membrane in Man. Protein Pattern, Inorganic Phosphate Binding and Transport: Comparison with other Species. *Renal Physiol* **7**: 65-71.
19. Biber, J. and Murer, H. (1985): Na-Pi Cotransport in LLC-PK₁ Cells: Fast Adaptive Response to Pi Deprivation. *Am J Physiol* **249**: C430-C434.
20. Caverzasio J. et al. (1985): Adaptation of phosphate transport in phosphate-deprived LLC-PK₁ cells. *Am J Physiol* **248**: F122-F127, 1985
21. Meghi, S. (1992): Bone Remodelling. *Brit Dent J* **172**: 235-242.
22. Donahue, H.J et al. (1988): Differential Effects of Parathyroid Hormone and its Analogs on Cytosolic Calcium Ion and cAMP Levels in Cultured Rat Osteoblast-like Cells. *J Biol Chem* **263**: 13522-13527.
23. Rosenbusch, J.P. et al. (1967): Parathyroid Hormone Effects on Amino Acid Transport into Bone Cells. *Endocrinology* **81**: 553-557.
24. Kream, B.E. et al. (1986): Hormone Regulation of Collagen Synthesis in a Clonal Rat Osteosarcoma Cell Line. *Endocrinology* **119**: 1922-1928.
25. Lian, J.B. et al. (1985): Studies of Hormonal Regulation of Osteocalcin Synthesis in Cultured Fetal Rat Calvariae. *J Biol Chem* **260**: 8706-8710.
26. Meyer, R.A. et al. (1989): X-linked Hypophosphatemia. *Sem Nephrol* **9**: 56-61.
27. Insogna, K.L. et al. (1983): Impaired Phosphorous Conservation and 1,25 dihydroxyvitamin D Generation during Phosphorous Deprivation in Familial Hypophosphatemic Rickets. *J Clin Invest* **71**: 1562-1569.
28. Glorieux, F.H. et al. (1976): Intestinal Phosphate Transport in Familial Hypophosphatemic Rickets. *Pediat Res* **10**:691-696.

29. Migeon, B.R. (1994): X-chromosome Inactivation: Molecular Mechanisms and Genetic Consequences. *TIG* 10: 230-235.
30. Gilbert, R.F. (1994): Developmental Biology. 4th edition, Sinauer Associates Inc. Publishers, Massachusetts, USA, 425-427.
31. Giannoukakis, N. et al. (1993): Parental Genomic Imprinting of the Human IGF2 Gene. *Nature Genet* 4: 98-101.
32. Machler, M. et al. (1986): X-linked Dominant Hypophosphatemia is Closely Linked to DNA Markers. *Hum Genet* 73: 271-275.
33. Econs, M.J. et al. (1992): Multilocus Mapping of the X-linked Hypophosphatemic Rickets Gene. *J Clin Endocrinol Metab* 75: 201-206.
34. Econs, M.J. et al. (1993): Flanking Markers Define the X-linked Hypophosphatemic Rickets Gene Locus. *J Bone Min Res* 8: 1149-1152.
35. Francis, F. et al. (1994): A YAC Contig Spanning the Hypophosphatemic Rickets Disease Gene (HYP) Candidate Region. *Genomics* 21: 229-237.
36. Econs, M.J. et al. (1994): Fine Structure Mapping of the Human X-linked Hypophosphatemic Rickets Gene Locus. *J Clin Endocrinol Metab* 79: 1351-1354.
37. The Hyp Consortium (1995): A Gene (PEX) with Homologies to Endopeptidases is Mutated in Patients with X-linked Hypophosphatemic Rickets. *Nat Gen* 11: 130-136.
38. Eicher, E.M. et al. (1976): Hypophosphatemia: Mouse Model for Human Familial Hypophosphatemic (Vitamin D-Resistant) Rickets. *Proc Natl Acad Sci* 73: 4667-4671.
39. Tenenhouse, H.S. et al. (1981): Intestinal Transport of Phosphate Anion is not Impaired in the Hyp (Hypophosphatemic) Mouse. *Biochem Biophys Res Commun* 100: 537-543.
40. Seino, Y. et al. (1982): 1,25-Dihydroxyvitamin D₃ Receptor in the X-linked Hypophosphatemic Mouse. *Endocrinology* 111: 329-331.
41. Meyer, R.A. et al. (1987): Evidence that Low Plasma 1,25-Dihydroxyvitamin D causes Intestinal Malabsorption of Calcium and Phosphate in Juvenile X-linked Hypophosphatemic Mice. *J Bone Min Res* 2: 67-82.
42. Giasson, S.D. et al. (1977): Micropuncture Study of Renal Phosphorous Transport in Hypophosphatemic Vitamin D Resistant Rickets Mice. *Pflugers Arch* 371: 33-38.

43. Bell, C.L. et al. (1988): Primary Cultures of Renal Epithelial Cells from X-linked Hypophosphatemic (Hyp) Mice Express Defects in Phosphate Transport and Vitamin D Metabolism. *Am J Hum Genet* **43**: 293-303.
44. Tenenhouse, H.S. et al. (1978): Renal Handling of Phosphate *In Vivo* and *In Vitro* by the X-linked Hypophosphatemic Male Mouse: Evidence for a defect in the Brush Border Membrane. *Kidney Int* **14**: 236-244.
45. Tenenhouse, H.S. et al. (1989): Effect of Phosphonoformic Acid, Dietary Phosphate and the Hyp Mutation on Kinetically Distinct Phosphate Transport Processes in Mouse Kidney. *Biochem Biophys Acta* **984**: 207-213.
46. Tenenhouse, H.S. et al. (1994): Renal Na⁺-phosphate Cotransport in Murine X-linked Hypophosphatemic Rickets. *J Clin Invest* **93**: 671-676.
47. Kos, C.H. et al. (1994): Localization of a Renal Sodium Phosphate Cotransporter Gene to Human Chromosome 5q35. *Genomics* **19**: 176-177.
48. Lobaugh, B. and Drezner, M.K. (1983): Abnormal Regulation of Renal 25-hydroxyvitamin D-1 α -hydroxylase Activity in the X-linked Hypophosphatemic Mouse. *J Clin Invest* **71**: 400-403.
49. Yamaoka, K. et al. (1986): Abnormal Relationship Between Serum Phosphate Concentration and Renal 25-hydroxycholecalciferol-1 α -hydroxylase Activity in X-linked Hypophosphatemic Mice. *Miner Electrolyte Metab* **12**: 194-198.
50. Nesbitt, T. et al. (1986): Abnormal Parathyroid Hormone Stimulation of 25-hydroxyvitamin D-1 α -hydroxylase Activity in the Hypophosphatemic Mouse. Evidence for a Generalized Defect in Vitamin D Metabolism. *J Clin Invest* **77**: 181-187.
51. Fukase, M. et al. (1984): Abnormal Regulation of 25-hydroxyvitamin D₃-1 α -hydroxylase Activity by Calcium and Calcitonin in Renal Cortex from Hypophosphatemic (Hyp) Mice. *Endocrinology* **114**: 1203-1207.
52. Econs, M.J. et al. (1991): Normal Calcitonin Stimulation of Serum Calcitriol in Patients with X-linked Hypophosphatemic Rickets. *J Clin Endocrin Metabol* **75**: 408-410.
53. Nesbitt, T. et al. (1987): Calcitonin Stimulation of Renal 25-hydroxyvitamin D-1 α -hydroxylase Activity in Hypophosphatemic Mice. *J Clin Invest* **79**: 15-19.
54. Nesbitt, T. and Drezner, M.K. (1990): Abnormal Parathyroid Hormone-related Peptide Stimulation of Renal 25-hydroxyvitamin D-1-hydroxylase in Hyp Mice: Evidence for a Generalized Defect of Enzyme Activity in the Proximal Convoluted Tubule.

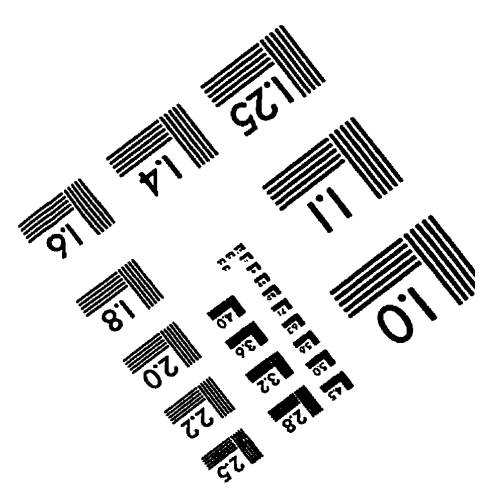
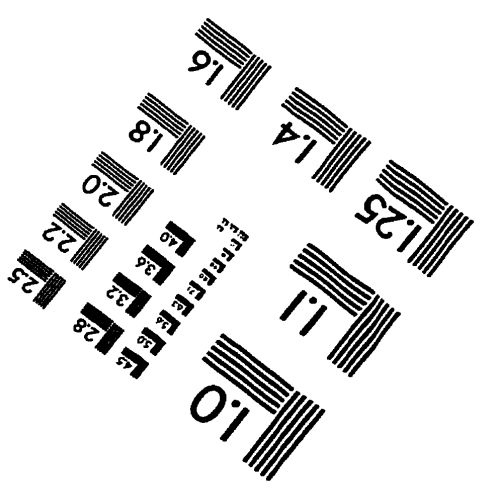
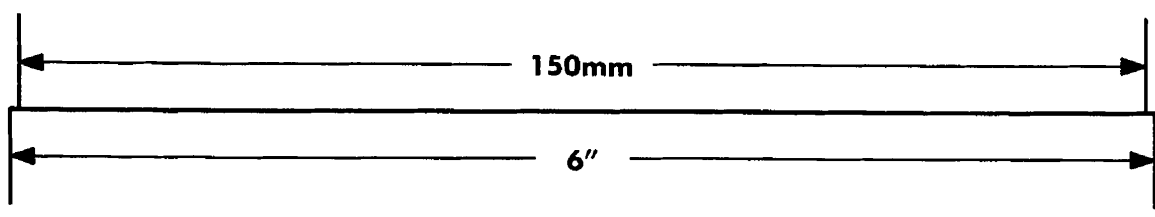
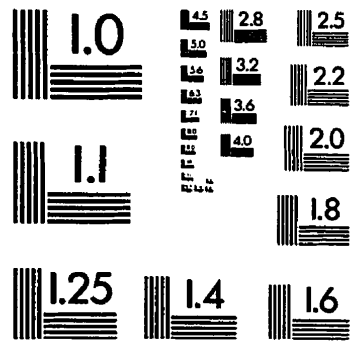
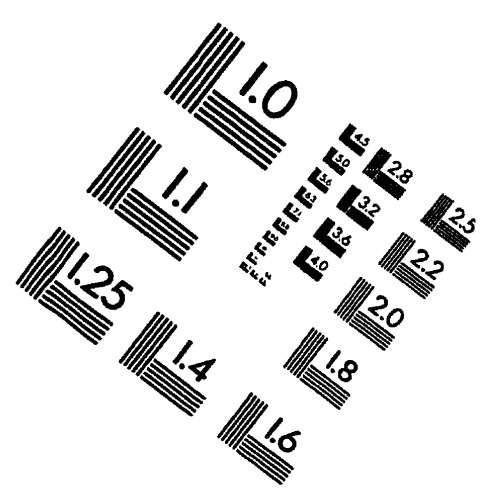
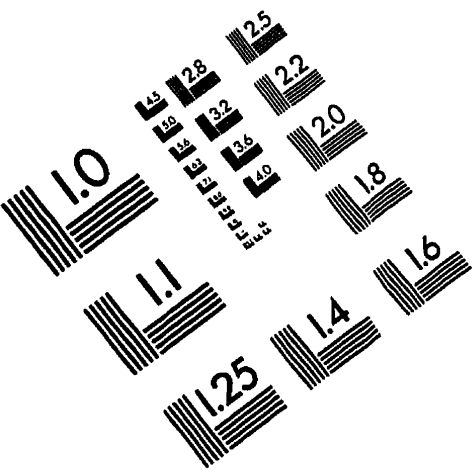
Endocrinology 127: 843-847.

55. Fukase, M. et al. (1984): Abnormal Regulation of 25-hydroxyvitamin D₃-1- α -hydroxylase Activity by Calcium and Calcitonin in Renal Cortex from Hypophosphatemic (Hyp) Mice. *Endocrinology* 114: 1203-1207.
56. Tenenhouse, H.S. et al. (1988): Increased Renal Catabolism of 1,25-dihydroxyvitamin D₃ in Murine X-linked Hypophosphatemic Rickets. *J Clin Invest* 81: 461-465.
57. Roy, S. et al. (1994): Increased Renal 25-hydroxyvitamin D₃-24-hydroxylase Messenger Ribonucleic Acid and Immunoreactive Protein in Phosphate Deprived Hyp Mice: A Mechanism for Accelerated 1,25-dihydroxyvitamin D₃ Catabolism in X-linked Hypophosphatemic Rickets. *Endocrinology* 134: 1761-1766.
58. Tenenhouse, H.S. and Jones, G. (1990): Abnormal Regulation of Renal Vitamin D Catabolism by Dietary Phosphate in Murine X-linked Hypophosphatemic Rickets. *J Clin Invest* 85: 1450-1455.
59. Tenenhouse, H.S. and Jones, G. (1987): Effect of the X-linked Hyp Mutation and Vitamin D Status on Induction of Renal 25-hydroxyvitamin D₃-24-hydroxylase. *Endocrinology* 120: 609-615.
60. Meyer, R.A. et al. (1989): The Renal Phosphate Transport Defect in Normal Mice Parabiosed to X-linked Hypophosphatemic Mice Persists after Parathyroidectomy. *J Bone Min Res* 4: 523-531.
61. Mandla, S. et al. (1990): Evidence for Protein Kinase C Involvement in the Regulation of Renal 25-hydroxyvitamin D₃-24-hydroxylase. *Endocrinology* 127: 2639-2647.
62. Boneh, A. and Tenenhouse, H.S. (1990): Protein Kinase C in Mouse Kidney: Effect of the Hyp Mutation and Phosphate Deprivation. *Kidney Intern* 37: 682-688.
63. Hruska, K.A. et al. (1987): Stimulation of Inositol Triphosphate and Diacylglycerol Production in Renal Tubular Cells by Parathyroid Hormone. *J Clin Invest* 79: 230-239.
64. Civitelli, R. et al. (1988): Parathyroid Hormone Elevates Inositol Polyphosphates and Diacylglycerol in a Rat Osteoblast-like Cell Line. *Am J Physiol* 255: E660-667.
65. Norman, A. et al. (1993): Demonstration that 1- β ,25-dihydroxyvitamin D₃ is an Antagonist of the Nongenomic but not Genomic Biological Responses and Biological Profile of the Three A-ring Diastereomers of 1- α ,25-dihydroxyvitamin D₃. *J Biol Chem* 268: 20022-20030.
66. Lieberherr, M. and Grosse, B. (1994): Androgens Increase Intracellular Calcium

- Concentration and Inositol 1,4,5-triphosphate and Diacylglycerol Formation via a Pertussis Toxin-sensitive G protein. *J Biol Chem* **229**: 7217-7223.
67. Bourdeau, A. et al. (1990): Rapid Effects of 1,25-dihydroxyvitamin D₃ and Extracellular Calcium on Phospholipid Metabolism in Dispersed Porcine Parathyroid Cells. *Endocrinology* **127**: 2738-2743.
68. Stryer, L. (1988): Biochemistry, 3rd edition, W.H. Freeman and Co., USA, 978-988.
69. Linder, M.E. and Gilman, A.G. (1992): G Proteins. *Sci Am* **267**: 56-65.
70. Taylor, C.W. (1992): The Role of G Proteins in Transmembrane Signaling. *Biochem J* **272**: 1-13.
71. Kurian, P. et al. (1992): Receptor Coupling to Phosphoinositide Signals. *Adv Exp Med Biol* **318**: 399-411.
72. Bligh, E.G. and Dyer, W.J. (1959): A Rapid Method for Total Lipid Extraction and Purification. *Can J Biochem* **37**: 911-917.
73. Bell, C.L. et al. (1985): Isolation and Culture of Murine Renal Proximal Tubule Cells: A System to Study Solute Transport in Mutants. *NY Acad Sci* **465**: 398-400.
74. Loch, C. and Antoine, R. (1995): A Proposed Mechanism of ADP-ribosylation Catalyzed by the Pertussis Toxin S1 Subunit. *Biochimie* **77**: 333-340.
75. Tenenhouse, H.S. and Henry, H.L. (1985): Protein Kinase Activity Inhibitor in Mouse Kidney: Effect of the X-linked *Hyp* Mutation and Vitamin D Status. *Endocrinology* **117**: 1719-1726.
76. Wali, R.K. et al. (1990): 1,25(OH)₂ Vitamin D₃ Stimulates Membrane Phosphoinositide Turnover, Activates Protein Kinase C, and Increases Cytosolic Calcium in Rat Colonic Epithelium. *J Clin Invest* **85**: 1296-1303.
77. Lieberherr, M. et al. (1985): A Functional Cell Surface Receptor is Required for the Early Action of 1,25-Dihydroxyvitamin D₃ on the Phosphoinositide Metabolism in Rat Enterocytes. *J Biol Chem* **264**: 20403-20406.
78. Cathewood, B.D. (1985): 1,25 Dihydroxycholecalciferol and Glucocorticosteroid Regulation of Adenylate Cyclase in an Osteoblast-like Cell Line. *J Biol Chem* **260**: 736-743.
79. Armbrecht, H.J. et al. (1984): Effect of PTH and 1,25(OH)₂ D₃ on Renal 25(OH) D₃ Metabolism, Adenylate Cyclase and Protein Kinase. *Am J Physiol* **246**: E102-107.

80. Martin, K.J. et al. (1994): Effect of U-73,122, an Inhibitor of Phospholipase C on Actions of Parathyroid Hormone in Opossum Kidney Cells. *Am J Physiol* **266**: F254-258.
81. Kiebzak, G.M. and Meyer, R.A. (1982): X-linked Hypophosphatemic Mice are not Sensitive to Parathyroid Hormone. *Endocrinology* **110**: 1030-1036.
82. Hruska, K.A. et al. (1989): Stimulation of Inositol Triphosphate and Diacylglycerol Production in Renal Tubular Cells by Parathyroid Hormone. *J Clin Invest* **79**: 230-239.
83. Coleman, D.T. and Bilezikian, J.P. (1990): Parathyroid Hormone Stimulates Formation of Inositol Phosphates in a Membrane Preparation of Canine Renal Cortical Tubular Cells. *J Bone Min Res* **5**: 299-306.
84. Civitelli, R. et al. (1988): PTH Elevates Inositol Polyphosphates and Diacylglycerol in Rat Osteoblast-like Cell Line. *Am J Physiol* **255**: E660-667.
85. Coleman, D.T. et al. (1991): Effects of Guanine Nucleotides and Parathyroid Hormone on Inositol 1,4,5-Triphosphate Metabolism in Canine Renal Cortical Tubular Cell Membranes. *J Bone Min Res* **6**: 599-607.
86. Korte, K. and Casey, M.L. (1982): Phospholipid and Neutral Lipid Separation by One-Dimensional Thin-Layer Chromatography. *J Chromatogr* **232**: 47-53.
87. Roe, M.W. et al. (1990): Assessment of Fura-2 for Measurements of Cytosolic Free Calcium. *Cell Calcium* **11**: 63-73.
88. Du, L. et al. (1997): cDNA Cloning of the Murine *Pex* Gene Implicated in X-linked Hypophosphatemia and Evidence for Expression in Bone. *Genomics* **36**: 22-28.
89. Strom, T.M. et al. (1997): *Pex* gene deletions in Gy and Hyp mice provide mouse models for X-linked hypophosphatemia. *Hum. Mol. Gen.* **6**: 165-171.

TEST TARGET (QA-3)



APPLIED IMAGE, Inc
1653 East Main Street
Rochester, NY 14609 USA
Phone: 716/482-0300
Fax: 716/288-5989

© 1993, Applied Image, Inc., All Rights Reserved